J Cell Sci. 2015 Aug 1; 128(15): 2938–2950.
doi: 10.1242/jcs.173807: 10.1242/jcs.173807
PMCID: PMC4540953
PMID: 26092939

Mitf is a master regulator of the v-ATPase, forming a control module for cellular homeostasis with v-ATPase and TORC1

Tianyi Zhang,[1,*§] Qingxiang Zhou,[1,§] Margret Helga Ogmundsdottir,[2] Katrin Möller,[2] Robert Siddaway,[3] Lionel Larue,[4] Michael Hsing,[5,‡] Sek Won Kong,[5] Colin Ronald Goding,[3] Arnar Palsson,[6] Eirikur Steingrimsson,[2,¶] and Francesca Pignoni[1,7,¶]

[1]Department of Ophthalmology, Center for Vision Research and SUNY Eye Institute, Upstate Medical University, Syracuse, 13210, NY, USA
[2]Department of Biochemistry and Molecular Biology, BioMedical Center, Faculty of Medicine, University of Iceland, Vatnsmyrarvegur 16, Reykjavik 101, Iceland
[3]Ludwig Institute for Cancer Research, Nuffield Department of Clinical Medicine, University of Oxford, Headington, OX3 7DQ, Oxford, UK
[4]Institut Curie, INSERM U1021, CNRS UMR3347, Normal and Pathological Development of Melanocytes, 91405, Orsay, France
[5]Informatics Program, Boston Children's Hospital, 300 Longwood Avenue, Boston, MA 02115, USA
[6]Life and Environmental Sciences, School of Engineering and Natural Sciences, University of Iceland, Vatnsmyrarvegur 16, Reykjavik 101, Iceland
[7]Departments of Neuroscience and Physiology, Biochemistry and Molecular Biology, Upstate Medical University, Syracuse, 13210, NY, USA
[*]Present address: Ben May Institute for Cancer Research, Chicago University, Chicago, IL, USA.
[‡]Present address: Vancouver Prostate Centre, 2660 Oak Street, Vancouver, British Columbia, Canada V6H 3Z6.
[§]These authors contributed equally to this work
[¶]Authors for correspondence (pignoniF@upstate.edu ;eirikurs@hi.is)

Received 2015 May 1; Accepted 2015 Jun 12.

ABSTRACT

The v-ATPase is a fundamental eukaryotic enzyme that is central to cellular homeostasis. Although its impact on key metabolic regulators such as TORC1 is well documented, our knowledge of mechanisms that regulate v-ATPase activity is limited. Here, we report that the *Drosophila* transcription factor Mitf is a master regulator of this holoenzyme. Mitf directly controls transcription of all 15 v-ATPase components through M-box cis-sites and this coordinated regulation affects holoenzyme activity *in vivo*. In addition, through the v-ATPase, Mitf promotes the activity of TORC1, which in turn negatively regulates Mitf. We provide evidence that Mitf, v-ATPase and TORC1 form a negative regulatory loop that maintains each of these important metabolic regulators in relative balance. Interestingly, direct regulation of v-ATPase genes by human MITF also occurs in cells of the melanocytic lineage, showing mechanistic conservation in the regulation of the v-ATPase by MITF family proteins in fly and mammals. Collectively, this evidence points to an ancient module comprising Mitf, v-ATPase and TORC1 that serves as a dynamic modulator of metabolism for cellular homeostasis.

KEY WORDS: MITF, TFEB, TORC1, Gut, Melanocytes, v-ATPase

INTRODUCTION

The vacuolar (H^+)-ATPase (v-ATPase) is an evolutionarily conserved holoenzyme that controls basic cellular processes in eukaryotic cells. As an ATP-dependent proton pump, it acidifies intracellular or extracellular compartments and generates electrochemical gradients, with profound consequences on lysosomal degradation, the transport of metabolites across gut epithelia and many other cellular processes (Allan et al., 2005; Marshansky et al., 2014). In lysosomal metabolism, the v-ATPase is a dual player; its proton pumping ability establishes the low pH required by degradative enzymes, whereas its ATPase activity is essential for the amino-acid-dependent activation of target of rapamycin complex 1 (TORC1; the kinase that links lysosomal degradation to the nutritional state of the cell). Interestingly, in mammalian cell lines, both negative (Settembre et al., 2011) and positive (Peña-Llopis et al., 2011) correlation of TORC1 activity with v-ATPase gene expression (the ATP6 genes) has been reported. Thus, the effect of TORC1 on the v-ATPase is unclear. However, in both cases, members of the MiT or MITF family of transcription factors have been implicated as

mediators of positive or negative regulation by TORC1 (Martina et al., 2012; Peña-Llopis and Brugarolas, 2011; Peña-Llopis et al., 2011; Roczniak-Ferguson et al., 2012; Settembre et al., 2011, 2012).

The four MiT family proteins in mammals, MITF, TFEB, TFE3 and TFEC, are basic helix-loop-helix leucine zipper (bHLH-Zip) transcription factors that control basic cellular processes in eukaryotes as well as tissue identity and differentiation in animal development (Steingrímsson et al., 2004). Recent studies in mammalian cell lines have implicated MITF, TFEB and TFE3 in the regulation of degradation pathways (Martina et al., 2012, 2014; Peña-Llopis and Brugarolas, 2011; Roczniak-Ferguson et al., 2012; Sardiello et al., 2009; Settembre et al., 2011, 2012). Expression profiling shows that these factors induce lysosomal and autophagy genes, with most of the targets containing the CLEAR element, a binding site for TFEB (Martina et al., 2012; Peña-Llopis and Brugarolas, 2011; Peña-Llopis et al., 2011; Palmieri et al., 2011; Sardiello et al., 2009). Interestingly, the nuclear versus cytoplasmic localization of MITF, TFEB, and TFE3 is controlled by the TORC1 kinase through phosphorylation. The mTOR-associated Rag GTPases can interact at an N-terminal motif present in all three MiT factors and promote their localization at the lysosome. Phosphorylation of the transcription factors by TORC1 then leads to their cytoplasmic sequestration by 14-3-3 proteins (Martina et al., 2012; Roczniak-Ferguson et al., 2012; Settembre et al., 2012). Alternatively, phosphorylation of TFEB by active TORC1 at a C-terminal serine-rich motif has been proposed to promote its nuclear translocation and activation (Peña-Llopis and Brugarolas, 2011; Peña-Llopis et al., 2011). Different cell culture conditions and the complication of dealing with multiple MiT family members might have contributed to this discrepancy. Nonetheless, the nature of this TORC1 regulation needs further study.

The invertebrate model organism *Drosophila melanogaster* offers two advantages. First, it provides a sophisticated genetic model to address questions *in vivo*, and second, it has a single MiT family factor. The gene *Mitf* (*CG43369*) is expressed broadly at a low level throughout the *Drosophila* life cycle, but is particularly enriched in the digestive system (Hallsson et al., 2004). Its physiological roles are unknown, due to a lack of loss-of-function analyses. Here, we identify Mitf as a master regulator of the major cellular v-ATPase through transcriptional control of all 15 subunits of the holoenzyme. Modulation of gene expression is direct and impacts upon holoenzyme activity, with profound consequences on all three metabolic regulators. We find that Mitf, the v-ATPase and TORC1 form a regulatory module that maintains the three factors in dynamic balance and potentially introduces an adaptive aspect to its regulation of metabolism. Interestingly, these Mitf functions appear to be conserved in human cells, pointing to an ancient Mitf/v-ATPase /TORC1 module for cellular homeostasis.

RESULTS

Mitf conservation with mammalian MiT transcription factors and function in the *Drosophila* gut

Although it is named Mitf (Hallsson et al., 2004), the fly protein is similarly related to all four mammalian family members. Phylogenetic analysis on selected species shows that the vertebrate genes form monophyletic groups, representing four orthologous gene families (with 89–99% bootstrap support) (Fig. 1A). Their phylogenetic emergence coincides with the whole genome duplications at the base, or during the early evolution, of the vertebrate clade (Holland et al., 1994; Ohno, 1999); the invertebrate MiT genes are clear outgroups (Fig. 1A). All of the proteins share the defining structural motifs, the bHLH-Zip (with particularly high conservation in the DNA-binding 'basic' domain; supplementary material Table S1A) as well as several confirmed or putative regulatory residues (supplementary material Table S1B) (Hallsson et al., 2007). An ancestral origin for some sites involved in phosphorylation, sumoylation and ubiquitylation, for example, S73, K182 and K201 (amino acid residues as per MITF isoform 4), is supported by the conservation of these motifs not only in the fly and vertebrate proteins but also in the selected representative of nematodes, primitive chordates, annelids and cnidarians. In regards to regulation by TORC1, the N-terminal SR-QL Rag-binding motif (present in TFEB, TFE3 and MITF, but not TFEC) is well conserved in fly and *Ciona intestinalis*, partially preserved in *Capitella teleta* and *Hydra vulgaris*, and apparently absent in the *Caenorhabditis elegans* protein; the C-terminal serine-rich motif (present in all four mammalian factors) is reasonably well conserved in fly but apparently absent in the other invertebrates (supplementary material Fig. S1B). Regardless, the presence of several regulatory or modification sites in multiple invertebrate and vertebrate proteins suggests a conservation of ancestral motifs and associated regulatory mechanisms.

To study the *Mitf* gene in *Drosophila*, we generated multiple reagents for loss-of-function and gain-of-function analysis (Fig. 1B). Although broadly expressed at a low level, *Mitf* mRNA is highly enriched in the gut (Hallsson et al., 2004). Accordingly, the reporter $Mitf^{2.2}$*-GFP* (Fig. 1B) showed expression in the late embryo and larval digestive system, including in the larval midgut, hindgut and Malpighian tubules (Fig. 1C). Given that only exogenous protein levels could be detected with the anti-Mitf antibody, we constructed a synthetic Mitf target, *4Mbox-GFP* (Fig. 1D), based on a mammalian reporter that responded to fly Mitf in cell culture (Hallsson et al., 2004). The *4Mbox-GFP* transgene was strongly induced in the larval hindgut and the Malpighian tubules (Fig. 1E,F), but not in the midgut (Fig. 1E), suggesting that unknown tissue-specific factors or the binding affinity of the *4Mbox* sites influenced regulation by Mitf *in vivo*. Nonetheless, *4Mbox-GFP* expression in hindgut and Malpighian tubules was indeed Mitf dependent, as shown by nearly absent expression in $Mitf^{TZ2}$*/Df(4)TZ* mutant larvae (Fig. 1G) or larvae with hindgut-targeted RNA interference (RNAi) (*byn-Gal4 UAS-*$Mitf^{RNAi}$) (Fig. 1H,I) (see supplementary material Table S2 for genotypes in all figures; supplementary material Fig. S1A–C for Gal4 patterns; and supplementary material Fig. S1D–G for RNAi validation). Consistent with reporter induction by

Mitf, the loss of *4Mbox-GFP* expression and the early larval lethality of *byn-Gal4 UAS-Mitf*^{RNAi} animals could be rescued by an RNAi-resistant genomic construct (*Mitf-rescue*$^{SI1\text{-}RES}$) (supplementary material Fig. S1E–G).

Thus, Mitf is active in the digestive system of *Drosophila* where it can function as a transcriptional activator and is required for organismal survival.

Mitf controls genes for all v-ATPase subunits

To understand Mitf function, we set out to identify genetic targets through gene expression profiling of loss and gain of Mitf. Mutant hindgut and Malpighian tubules provided loss-of-function tissue; gain-of-function was obtained by overexpressing Mitf in the wing disc epithelium (*nub-Gal4 UAS-Mitf*; Fig. 2A) where endogenous Mitf levels were low. We then compared the gene set upregulated by Mitf overexpression in the wing disc (*nub-Gal4 UAS-Mitf* versus *nub-Gal4*) to the gene set downregulated in *Mitf* mutant hindgut plus Malpighian tubules (*Mitf*^{TZ2}*/Df(4)TZ* larvae) (Fig. 2B). A total of 85 genes were both upregulated in wing and downregulated in hindgut plus Malpighian tubules (Fig. 2C; supplementary material Table S3A). Ontological analysis of these 85 genes uncovered a striking enrichment for *Vha* loci encoding the 15 subunits of the fly v-ATPase complex. Of 33 *Vha* genes, 14 were regulated by Mitf (≥1.4 fold; $P \leq 0.01$) (Fig. 2D; supplementary material Table S3B). One more subunit gene, *Vha36-1*, was robustly downregulated in mutant hindgut plus Malpighian tubules (3.8 fold; $P < 0.01$) but modestly upregulated in the wing (1.3 fold; $P < 0.01$). Strikingly, this collection of 15 Mitf targets codes for a complete set of v-ATPase components (Fig. 2D); for subunits with multiple loci, the one most broadly and highly expressed responded to Mitf (Chintapalli et al., 2013).

For validation, we investigated the regulation of seven *Vha* genes *in vivo*, five encoding components of the cytoplasmic, ATP-hydrolyzing V1 sector [*Vha13* (V1G), *Vha26* (V1E), *Vha55* (V1B), *Vha68-2* (V1A), *VhaSFD* (V1H)] and two encoding subunits of the transmembrane, proton-transporting V0 sector [*Vha16-1* (V0c), *VhaAC39-1* (V0d)] (designations in parentheses refer to the encoded subunit type; see Fig. 2D). The expression of enhancer traps (*Vha55–*, *Vha26–*, and *Vha68-2–*lacZ), gene traps (*Vha13–*, *VhaSFD–* and *Vha16-1–*GFP) and mRNA (*VhaAC39-1*) were strongly upregulated in wing discs with exogenous Mitf (Fig. 2E,F; supplementary material Fig. S2A), reflecting the pattern of the Gal4 driver used (*en-Gal4*, *Ser-Gal4* or *dpp-Gal4*). Conversely, expression of the same enhancer traps and gene traps lines was lost in Mitf-deficient larvae. *Mitf*^{TZ2}*/Df(4)TZ* mutant larvae showed loss of expression in midgut, hindgut and Malpighian tubules (Fig. 2G; supplementary material Fig. S2B); whereas *byn-Gal4 UAS-Mitf*^{RNAi} larvae showed loss of expression specifically in the hindgut (where byn-Gal4 is expressed) (Fig. 2H; supplementary material

Fig. S2C).

Thus, Mitf is both required and sufficient for induction of *Vha* genes. Remarkably, Mitf drives expression of one gene for every component of the complex, specifically coordinating the expression of a full set of subunits of the major v-ATPase.

Mitf regulates v-ATPase activity and lysosomal metabolism

To explore the *in vivo* consequences of subunit co-regulation, we probed for changes in holoenzyme activity and lysosomal metabolism, a cellular process heavily dependent on both MiT-type factors and the v-ATPase (Sardiello et al., 2009; Marshansky et al., 2014).

Several experiments indicated that increased *Vha* gene expression leads to increased v-ATPase activity. Firstly, in genetic interaction tests, loss-of-function alleles of several *Vha* genes behaved as a dominant suppressor of the abnormal wing phenotype of *dpp-Gal4 UAS-Mitf* flies. Of seven *Vha* genes tested, all but one suppressed the phenotype (Fig. 3A; supplementary material Fig. S2D), strongly suggesting that a reduction in holoenzyme restored normal wing development. Secondly, expression of a Vha55–GFP fusion protein, whose stability has been linked to complex assembly (Fig. 3B) (Du et al., 2006), increased when Mitf was co-expressed (Fig. 3C,D; supplementary material Fig. S2E). This is consistent with stabilization of the fusion protein as a result of increased v-ATPase assembly. Thirdly, upon overexpression in the wing epithelium (*en-Gal4 UAS-Mitf*), Mitf led to an expansion of the acidic compartments in wing cells, as detected with the acidotropic dye LysoTracker (Fig. 3E). Collectively, these data provided evidence of an effect of Mitf on the level of active holoenzyme.

The LysoTracker experiment also suggested that there was a possible expansion of the lysosomal compartment. Indeed, the Mitf-induced wing phenotype was also suppressed by depletion of lysosomal components, including *Cp1*, *Rab2*, *spin* and *Lamp1* (Fig. 3F), suggesting a role for lysosomal metabolism in the disruption of wing development. To visualize the lysosomal compartment in the wing epithelium, we used the fusion proteins Rab7–YFP and Spin–GFP, which preferentially mark early and mature lysosomes, respectively (Marois et al., 2006; Sweeney and Davis, 2002). In wing discs expressing Mitf in the posterior half (*en-Gal4 UAS-Mitf*) and Rab7–YFP constitutively throughout the epithelium (*tub-Rab7-YFP*), we observed a dramatic increase in Rab7–YFP staining in the posterior as compared to the anterior region (Fig. 3G). Interestingly, Mitf like Rab7–YFP, showed a punctate distribution typical of vesicles and in many cases the punctate signals overlapped, suggesting an association of fly Mitf with lysosomes that is reminiscent of the mammalian factors (Fig. 3G, inset) (Martina et al., 2012; Roczniak-Ferguson et al., 2012; Settembre et al., 2012). Similarly, in

dpp-Gal4 UAS-spin-GFP wing discs (without exogenous Mitf), the Spin–GFP fusion protein localized apically, as expected for mature lysosomes, in cells at the center of the *dpp-Gal4* stripe (Fig. 3H, left panel). In contrast, when MITF was also expressed (*dpp-Gal4 UAS-spin-GFP UAS-Mitf*), we detected increased staining throughout the cell body (Fig. 3H, right panel). Thus, the Rab7–YFP and the Spin–GFP-positive compartments appear to be expanded in tissue with exogenous Mitf, suggesting an enhancement of lysosome biogenesis.

To confirm that these phenotypes did not reflect solely a gain-of-function effect of Mitf, we then focused on the hindgut. In the wt hindgut, Rab7–YFP (*tub-Rab7-YFP*) and Spin–GFP (*byn-Gal4 UAS-Spin-GFP*) displayed low expression (Fig. 3I,J, left panels), reflecting normal levels of lysosomal activity. Strikingly, RNAi-mediated knockdown of Mitf (*byn-Gal4 UAS-Mitf*^{RNAi}) also resulted in a dramatic increase in Rab7–YFP and Spin–GFP staining (Fig. 3I,J, right panels), thereby producing an effect similar to exogenous Mitf in the wing. However, a failure to produce functional lysosomes, a process that requires the v-ATPase, can also result in accumulation of dysfunctional vesicles in the cytoplasm (Pulipparacharuvil et al., 2005). Therefore, we used an available lysosomal-activity sensor, *tub-GFP-Lamp1* (Akbar et al., 2009; Pulipparacharuvil et al., 2005), to assess lysosomal function in both Mitf-overexpressing wings and Mitf-mutant guts. The *tub-GFP-Lamp1* sensor is based on the Lamp1 protein (an abundant component of the lysosomal membrane) and encodes a GFP–Lamp1 fusion protein engineered so that the GFP moiety is released in the lumen to be quickly degraded by lysosomal peptidases. Thus, the GFP protein is hardly detectable in functioning lysosomes, whereas it accumulates in dysfunctional organelles (Akbar et al., 2009; Pulipparacharuvil et al., 2005). Consistent with increased acidification (Fig. 3E), the GFP protein was weakly detected in Mitf-expressing wings, which appeared similar to no-Mitf controls (Fig. 3K). By contrast, GFP expression increased greatly in Mitf^{RNAi}-expressing hindgut cells as compared to Gal4-only controls (Fig. 3L), indicating that lysosomes are impaired in the Mitf-mutant gut. These results support a model whereby Mitf gain and Mitf loss induce increases of lysosomal vesicles through two different mechanisms: Mitf gain does so by overall upregulation of lysosomal biogenesis, whereas Mitf loss impairs lysosomal function with consequent failure of turnover.

Taken together, this evidence confirms that Mitf is involved in lysosomal metabolism in fly and, more importantly, supports a key role for Mitf in regulating v-ATPase activity *in vivo*.

Mitf directly regulates v-ATPase subunit genes

To explore how Mitf controls the *Vha* genes, we searched for cis-regulatory motifs enriched in the 15 controlled loci, but not the 18

unresponsive ones. Remarkably, a MEME-based search for over-represented motifs within the putative regulatory DNA of the 15 Mitf-responsive genes identified a 10-bp sequence [(T/G)GTC(A/T)TGTGA; Fig. 4A; E-value 2.7×10^{-8}] that was strikingly similar to the CLEAR element (GTCACGTGAC) and the M-box (CATGTG) bound by mammalian TFEB and MITF, respectively (Sardiello et al., 2009; Budd and Jackson, 1995). Given that fly Mitf can robustly induce expression from the mammalian M-box, for example, *4Mbox-GFP in vivo* (Fig. 1D–F) and *MBpLuc in vitro* (Hallsson et al., 2004), we considered this newly identified 10-bp element a true binding site of fly Mitf.

Using Target Explorer and Vista, we then searched for such sites within all 33 *Vha* genes (225,353 bp, including 2 kb of flanking DNA on each side of transcription unit) and assessed their evolutionarily conservation. A total of 55 matches were present and 33 were evolutionarily conserved (Fig. 4B; supplementary material Table S4). Strikingly, all 33 conserved sites mapped to non-coding regions of the Mitf-regulated *Vha* genes (13 of 15 genes) (Fig. 4B). A slight relaxation of the matrix cut-off score or use of a shorter 8-bp consensus identified evolutionarily conserved sites in the remaining two putative Mitf targets, *VhaM9.7-b* and *VhaPPA1-1*, but not in any other *Vha* genes (supplementary material Table S4). In short, evolutionarily conserved Mitf-binding sites were present in all 15 regulated *Vha* genes, but in none of the 18 non-regulated *Vha* loci.

To confirm that such sites were indeed functional, we carried out chromatin immunoprecipitation (ChIP) and expression reporter analysis *in vivo*. We randomly selected five Mitf-regulated *Vha* genes and confirmed by ChIP that the sites were indeed occupied by Mitf–Myc *in vivo* (Fig. 4C). We then selected two genes (*Vha68-2* with six consensus sites in an intron, and *Vha13* with one site near the transcription start) and constructed GFP reporters with wild-type and mutated sequences (Fig. 4D,G). Wild-type *Vha68-2-GFP* and *Vha13-GFP* reporters were strongly expressed in the larval gut, whereas the mutated ones were not (Fig. 4E,F,H,I).

Taken together, these data support the view that, in *Drosophila*, a set of *Vha* loci constitutes a synexpression group directly controlled by Mitf.

An Mitf/v-ATPase/TORC1 regulatory loop for cellular homeostasis

An important role of the v-ATPase in both vertebrates and flies is regulating the activity of TORC1, which in turn has been shown to affect the subcellular localization of TFEB in cell lines. In this context, our discovery that Mitf regulates the activity of the v-ATPase in *Drosophila* suggested the existence of a regulatory loop involving Mitf, the v-ATPase and TORC1.

To explore this, we first investigated, in the large cells of the salivary glands, whether TORC1 controls fly Mitf localization. The fly protein shows conservation of the N-terminal Rag-interaction site (SR-QL) as well as the C-terminal serine-rich motif (SS-RS) identified in the vertebrate proteins (Fig. 5A; supplementary material Table S1B) (Martina and Puertollano, 2013; Peña-Llopis et al., 2011). First, we probed which side of the Mitf protein was involved in subcellular localization, knowing that full-length exogenous Mitf is detected more in the cytoplasm than the nucleus of expressing cells (Fig. 5A,A′). Interestingly, we did not detect any change in protein distribution after deleting the serine-rich region, $Mitf^{DelC1}$ (Fig. 5A′). By contrast, an N-terminal truncated protein lacking the Rag-interaction motif, $Mitf^{DelN1}$, was entirely nuclear (Fig. 5A′). Second, we investigated the regulation of the wild-type protein by TORC1. A reduction in the negative TORC1 regulators (Gig or TSC1) resulted in increased cytoplasmic staining (Fig. 5B), and, conversely, loss of positive regulators (the Rags or Raptor) resulted in increased nuclear signal (Fig. 5B; supplementary material Fig. S3A,A′). In short, nuclear versus cytoplasmic localization of Mitf correlated with conditions for lower or higher TORC1 activity, respectively. Consistent with these observations, loss of the cytoplasmic anchor proteins 14-3-3 also resulted in nuclear staining (supplementary material Fig. S3A,A′) and the Mitf-induced wing phenotype was suppressed by enhancing TORC1 activity; achieved through depletion of negative regulators, e.g. Gig (TSC2 in mammals) or TSC1, and enrichment of positive components, e.g. RagC-D (supplementary material Fig. S3B). Finally, we turned to a well-characterized physiological setting for TORC1 modulation, specifically starvation-induced inactivation of TORC1 in fly salivary glands cells (Mauvezin et al., 2014). In this background, we also detected a shift of Mitf to the nucleus (supplementary material Fig. S3C). Thus, in the fly, TORC1 functions as a negative regulator of Mitf activity by cytoplasmic sequestration.

These results confirmed the last segment of a regulatory loop that involves Mitf, the v-ATPase and TORC1. To demonstrate the existence of this loop *in vivo*, we sought to show that modulation of any one segment had repercussions further around the loop. Thus, we predicted that: (1) a decrease in v-ATPase would induce a shift of Mitf protein into the nucleus; (2) an increase in Mitf would affect its own intracellular localization; and, (3) an increase in Mitf would lead to a v-ATPase-dependent increase in TORC1 activity. Firstly, we looked at the effect of knockdown of *Vha* genes on Mitf protein localization. Expression of transgenic RNAi against either *VhaSFD* or *Vha68-2* induced a strong shift of Mitf protein into the nucleus of salivary glands cells (compare nuclear localization in *dpp-Gal4 UAS-Mitf* versus *dpp-Gal4 UAS-Mitf UAS-Vha*^{RNAi} in Fig. 5C,C′). Secondly, we used an ‘inactive’ Mitf protein, *UAS-*$Mitf^{DelR}$ (supplementary material Fig. S1H), defective in DNA-binding (Morii et al., 1994), to look at the effect of functional Mitf on its own localization. Interestingly, the non-functional $Mitf^{DelR}$ protein was found distributed through the cytoplasm and the nucleus of salivary glands cells more uniformly than wild-type Mitf, presumably reflecting the level of TORC1 activity in unperturbed salivary

glands (Fig. 5D, left panels). Strikingly, after co-expression of wild-type exogenous Mitf, the Mitf proteins were still detected in the cytoplasm but no longer in the nucleus (Fig. 5D, right panels). Thus, the activity of Mitf as a transcription factor appeared to promote its own cytoplasmic sequestration, a phenomenon consistent with increased TORC1 activity in response to activation of v-ATPase genes by wild-type Mitf. Thirdly, we relied on phosphorylation of the TORC1 target S6 kinase (S6K), a reporter of TORC1 activity (Burnett et al., 1998; Isotani et al., 1999), to probe the relationship between Mitf levels and the TORC1 complex. Using an antibody specific for phosphorylated S6K (pS6K), we compared the level of pS6K in cells expressing Gal4-only (*dpp-Gal4* control), expressing Mitf in an otherwise wild-type background (*dpp-Gal4 UAS-Mitf*) and expressing Mitf in a v-ATPase-compromised background (*dpp-Gal4 UAS-Mitf UAS-VhaSFD*^{RNAi}). Consistent with upregulation of TORC1 activity by Mitf through the v-ATPase, the level of pS6K increased with Mitf-expression (*dpp-Gal4* versus *dpp-Gal4 UAS-Mitf*) in a v-ATPase-dependent way (*dpp-Gal4 UAS-Mitf UAS-VhaSFD*^{RNAi}) (Fig. 5E).

In conclusion, these data show that Mitf, the v-ATPase and TORC1 are organized into a homeostatic loop (Fig. 5F) that regulates the activity of each of these factors and maintains them in a dynamic balance.

Conservation of v-ATPase regulation in human cells

To investigate the regulation of v-ATPase genes in mammals, we looked at MiT-family factors and v-ATPase (ATP6) genes in the melanocytic lineage, in which MITF is recognized as a master regulator of cell identity and differentiation (Steingrímsson et al., 2004).

Gene expression analysis of both MiT and v-ATPase genes in 24 human melanoma cell lines uncovered a strong correlation between the level of endogenous MITF transcripts and the expression of 19 of 23 ATP6 loci tested (Fig. 6A; supplementary material Table S5A). The median Kendall correlation was 0.64, with only four outliers close to 0 (Wilcoxon V=224, $P<0.0001$). As the correlation was specific to MITF, this suggested that MITF (and not other family members) might contribute significantly to the regulation of ATP6 genes in this cell type. Interestingly, this positive correlation was also present (albeit weaker) in the melanoma data set from the Cancer Genome Atlas (TCGA) (V=226, $P=0.006$; Fig. 6B; supplementary material Table S5B,C). The weaker correlation values likely reflect the genetic heterogeneity and histological complexity of tumors. Importantly, as in the cell lines, the positive correlation in tumors was specific for MITF (Fig. 6B; supplementary material Table S5B). Taken together, these finding suggested a strong link between v-ATPase genes and MITF expression.

To assess whether this correlation reflected a direct regulation of ATP6 genes by MITF, we performed ChIP-seq on a human 501Mel melanoma cell line that stably expresses HA–MITF at comparable levels to the endogenous gene (supplementary material Fig. S4A). Manual inspection of our ChlP-Seq data revealed MITF bound to many lysosomal genes with or without previously identified CLEAR elements (supplementary material Fig. S4B,C; supplementary material Table S6A) (Sardiello et al., 2009). More importantly, MITF-binding peaks were also found at a majority of ATP6 loci (20 of 25; P=0.002) (Fig. 6C-C′; supplementary material Table S6B), confirming and extending previous findings by Strub et al. (2011). Strikingly, 19 of the v-ATP6 genes bound by MITF showed positive correlation in the melanoma lines and only one gene (V1E2) did not (Table 1). This association between MITF–ATP6 binding in the ChIP-seq study and MITF–ATP6 correlation in the expression study is significant (Fisher's exact, P=0.0001).

Importantly, we also investigated whether this relationship was restricted to melanoma cells or could also be observed in the parental cell type, the melanocyte. For this, we analyzed data from a previous ChIP-seq study of endogenous MITF in primary human melanocytes (Webster et al., 2014). Among 6086 genes bound by MITF (out of 21,000 genes tested), we found a non-random distribution of 16 bound and 10 unbound v-ATPase loci (P<0.001) (supplementary material Table S6C). Binding occurred largely at sites identified in our melanoma study (supplementary material Table S6C), suggesting that MITF regulates these targets in both primary cells and cell lines. In addition, reduction of MITF expression in 501Mel cells to approximately one-third of normal levels (siMITF; Fig. 6D,D′) resulted in reduced expression for most genes bound in both melanoma cells and melanocytes (10 of 15 tested) (Fig. 6D″; Table 1). Taken together this evidence supports a model whereby the ATP6 genes are extensively and directly regulated by MITF in cells of the melanocytic lineage.

Finally, we asked whether regulation of v-ATPase genes by MITF also had an impact on TORC1. Thus, we generated two melanoma cell lines with inducible MITF and assessed the activity of TORC1, through phosphorylation of S6K, with and without treatment. In both cases, we observed an increase in phospho-S6K levels in response to MITF induction (Fig. 6E), strongly suggesting that, as in flies, increased MITF enhances TORC1 activity.

Thus, in the melanocytic lineage, MITF likely functions as an important modulator of v-ATPase and TORC1 activity.

DISCUSSION

The role of the v-ATPase as a fundamental regulator of metabolism is well documented and is underscored by its requirement in all eukaryotic cells (Marshansky et al., 2014). Understanding its regulation and how this ties to major metabolic pathways is crucial to

decoding the complex mechanisms of cellular homeostasis. This study shows that *Drosophila* Mitf plays a major role in regulating v-ATPase activity. Regulation is at the transcriptional level and direct, through cis sites generally located just upstream of the promoter or in a large early intron of each subunit-encoding *Vha* locus. Strikingly, 15 *Vha* genes appear to be organized into an Mitf-regulated synexpression group that ensures co-production of all components of the major v-ATPase. Through this mechanism, Mitf functions as a master regulator of the holoenzyme in the digestive system and other fly tissues.

Concerted expression of v-ATPase loci has also been observed in vertebrates but the genetic and molecular mechanisms mediating this synexpression are largely unknown (Holliday, 2014; Lee, 2012; Nelson et al., 2000). Whereas the fly has a single Mitf gene, the situation in mammals is more complex due to the presence of TFEB and TFE3. Nonetheless, in human melanoma cells, and most likely in melanocytes, MITF appears to directly regulate a set of ATP6 genes encoding all the main v-ATPase subunits. Fifteen ATP6 genes (encoding the 13 holoenzyme subunits and 1 accessory protein) are bound in both melanoma cells and primary melanocytes; among these, all show expression correlation with MITF in cell lines and most are downregulated in response to the partial silencing of MITF in cell culture (Table 1). We consider these 15 ATP6 genes the most likely targets of direct regulation by MITF in melanoma and melanocytes (Table 1). The remaining 10 loci show variable effects (with only one bound in melanocytes). These might include genes that are targets of other MiT factors in other tissues and can respond to MITF when it is overexpressed (as is often the case in melanoma tumors). In fact, it is likely that TFEB and TFE3 play a similar role to MITF in controlling most of the ATP6 loci in HeLa cells and ARPE-19 cells, respectively. Further analyses of these TFE factors and ATP6 genes in these cell lines will show whether this is the case.

In *Drosophila* and other insects, the v-ATPase works at the plasma membrane of cells lining gut and Malpighian tubules to regulate pH, energize ion transport and modulate fluid secretion (Wieczorek et al., 2009). In the developing epithelia of eye, wing and in the ovary, pH modulates the activity of internalized receptors such as Notch (Yan et al., 2009; Vaccari et al., 2010); hence, v-ATPase activity has repercussions on signaling. In wing discs, mutations in *VhaM8.9* can cause planar cell polarity defects, in addition to disrupting endosomal trafficking (Hermle et al., 2013). Whereas most of these functions would likely be affected in Mitf mutants, some v-ATPase subunits also fulfill specialized roles (Hiesinger et al., 2005). In the latter case, the influence of Mitf would depend on whether the specific subunit is under Mitf control and, if not, on whether the holoenzyme is the agent. Ultimately, many of these functions are essential for life and thus explain the lethality of *Mitf* mutant alleles.

In mammals, the v-ATPase plays essential roles in a broad range of processes that are regulated by one or other MiT family member.

The v-ATPase is essential for the proper function of melanosomes and many melanosome genes, in addition to ATP6 genes, are under MITF control. The v-ATPase also contributes to bone remodeling in osteoclasts, a cell type that expresses, and depends on MITF, TFEB and TFE3 for normal function (Scimeca et al., 2000; Blair et al., 1989; Udagawa et al., 1992). Interestingly, double knockout of the *Tfe3* and *Mitf* genes in mouse leads to osteopetrosis (Steingrimsson et al., 2002). The v-ATPase has also been found at the plasma membrane of cancer cells, from where it promotes alkalization of the cytoplasm and acidification of the tumor micro-environment, and this activity was recently linked to the emergence of distant metastases in melanoma (Nishisho et al., 2011). Further studies will elucidate the exact relationship between MiT factors and the v-ATPase in these contexts.

Importantly, in both vertebrates and *Drosophila*, the v-ATPase mediates the activation of TORC1 at the lysosomal membrane in response to amino acids (Zoncu et al., 2011), thereby downregulating lysosomal metabolism. Hence, the v-ATPase can have a negative influence on the lysosome even though it promotes lysosomal function through acidification (Mindell, 2012; Vaccari et al., 2010; Zoncu et al., 2011). In *Drosophila*, exogenous Mitf leads to increased TORC1 activity and promotes sequestration of Mitf back to the cytoplasm, whereas decreased v-ATPase gene dosage results in more nuclear Mitf as well as lower TORC1 function (Fig. 5). In 501Mel cells, exogenous MITF can also increase TORC1 activity (Fig. 6). Although the predominant isoform of MITF in melanocytes does not have the Rag-binding sites, other isoforms do, as do TFEB and TFE3. Hence, the regulatory loop is most likely conserved in mammals and functions in many cell types.

Most importantly, Mitf does not merely execute a pro-lysosomal program when freed from TORC1-induced sequestration. Through the v-ATPase, Mitf feeds back onto TORC1 to promote and limit the activity of these important metabolic regulators. The Mitf/v-ATPase/TORC1 regulatory loop adjusts the activity of all three players offering a mechanism for continuously balancing metabolic pathways as the nutritional state of the cell fluctuates. In addition, this could confer an adaptive feature to the module. In this model (supplementary material Fig. S4D), the level of v-ATPase, present at the lysosome, would sensitize or desensitize the nutritional sensing mechanism to changes in amino acid levels, thereby priming the system to reset at a new normal through TORC1 reactivation or inactivation. Such mechanism would impose a limit on upregulation of catabolism under low nutrient conditions, and an upper limit on active TORC1 and its promotion of anabolic pathways when nutrients are abundant (supplementary material Fig. S4D). Interestingly, cell culture experiments show that prolonged starvation reactivates TORC1 (Yu et al., 2010); here, the loop offers a potential molecular mechanism for this effect. Evolutionarily, the Mitf/v-ATPase/TORC1 regulatory module might have conferred a selective advantage by fine-tuning the nutrient-sensing mechanism to maintain metabolism within an optimal range in an ever-changing environment; an advantage particularly important for unicellular organisms or for cell types that require more precise

metabolic regulation.

Drosophila provides an excellent metazoan model to investigate the molecular mechanisms for co-regulation of v-ATPase subunits as well as the contribution of Mitf to the maintenance of cellular homeostasis. It will be also important to investigate how different members of the MiT family participate in these processes in different cell types under different physiological conditions and what impact they have on cellular homeostasis in health and disease.

MATERIALS AND METHODS

Evolutionary analysis

Sequences were obtained from Ensembl and Orthodb (Waterhouse et al., 2013) or by Blast to Genbank and model organism databases. Longest coding sequences and all extra exons were used in bioinformatic analyses. Protein alignment was performed with Muscle and Clustal omega (Sievers and Higgins, 2014), and manually curated in less conserved regions. MEGA6 (Tamura et al., 2013) was used to build phylogenetic trees with maximum likelihood (1000 bootstraps) and w/freq models (Jones et al., 1992). The tree with the highest log likelihood (−6386.1370) was reported, using an initial tree obtained automatically by applying Neighbor-Join and BioNJ algorithms to a matrix of pairwise distances estimated using a JTT model, and selecting the topology with superior log likelihood value. A discrete gamma distribution was used to model evolutionary rate differences among sites [five categories (+*G*, parameter=0.8871)]. A total of 381 positions were in the final dataset screened for conservation of motifs and specific residues.

Genetics

Crosses were at 25°C, unless specified here or in supplementary material Table S2. *byn-Gal4 UAS-Mitf*$^{RNAi\text{-}VDRC}$ animals were reared at 18°C to improve survival. Stocks are listed in supplementary material Table S7; genotypes used in each figure panel are in supplementary material Table S2. Different Gal4s were often used; results were consistent across drivers. The *Df(4)TZ*^{DC}, *Mitf*$^{KOw+}$ chromosome resulted from site-directed mutagenesis but contains a ∼100 kb deletion that removes *Dyrk3* and *Caps* in addition to the *Mitf* knockout. *Df(4)TZ*^{DC}, *Mitf*$^{KOw+}$ was used in standard ethyl methanesulfonate (EMS) mutagenesis to isolate lethals; two *Mitf* alleles were identified and characterized by single-embryo PCR and sequencing, and carry nonsense mutations Q152X and R292X, respectively (A isoform). The following constructs were generated: *4Mbox-GFP*; *Mitf2.2-eGFP*; *UAS-Mitf*$^{RNAi\text{-}TZ1\text{-}3}$ and *UAS-*

Mitf$^{RNAi\text{-}TZ4\text{-}8}$; *UAS-Mitf* expression constructs (wild-type, mutant and truncated; tagged and untagged; and without 5′ and 3′ UTRs for higher expression). For the *Mitf-rescue*^{SI1} (*Mitf* rescue Short Intron 1) and *Mitf-rescue*$^{SI1\text{-}RES}$ (*Mitf* rescue Short Intron 1 resistant), the constructs lack a very large first intron that contains repetitive DNA. For *Mitf-rescue*$^{SI1\text{-}RES}$, a 500-bp sequence targeted by *UAS-Mitf*$^{RNAi\text{-}VDRC}$ was obtained with silent nucleotide changes (Integrated DNA Technologies). For the *Vha-GFP* reporters, a 670 bp promoter region of *Vha13* and a 980 bp first intron of *Vha68-2* were cloned into pStinger-GFP (for*Vha13*) or pHStinger-GFP (for*Vha68-2*) (Barolo et al., 2000). Other vectors used were pWIZ (Lee and Carthew, 2003); pUASTattB, pCaspeR (Thummel and Pirrotta, 1991). Details are available upon request. All primers used are in supplementary material Table S8. w^{1118} stocks were injected in-house for site-directed or for P-element insertion.

Histology

Standard antibody, β-galactosidase, *in situ* and LysoTracker protocols were used (Juhasz and Neufeld, 2008). Anti-Mitf antibody was generated against full-length protein in guinea pig (Pocono Rabbit Farm). In salivary glands, >500 cells from six salivary glands were scored per genotype. Other primary antibodies used were: mouse anti-Dlg (1:100, DSHB), rabbit anti-GFP (1:1000, Invitrogen), rabbit anti-β-galactosidase (1:1000, Cappel), rat anti-Elav (1:100, DSHB), mouse anti-Myc (1:1000, Invitrogen) and rabbit anti-HA (1:100, Santa Cruz Biotechnology). Cy2-, Cy3-, or Cy5-conjugated secondary antibodies (Jackson Immuno Research Laboratories) used at 1:200. Imaging was performed with a Zeiss LSM510 scanning confocal/two-photon, Leica DM5500Q confocal microscope. *GFP* and *VhaAC39-1* probes were generated with the DIG RNA Labeling Kit (Roche). DIC imaging was performed with a Leica DM5500Q microscope with a DFC300FX digital camera.

Microarray

Hindguts and Malpighian tubules from L3 w^{1118} or *Mitf* mutant larvae (w^{1118}; $Mitf^{TZ2}/Df(4)TZ^{DC}$, $Mitf^{KOw+}$) and wing discs from L3 *nub-Gal4* or *nub-Gal4 UAS-Mitf* (CDS3) larvae were dissected and processed for RNA. Triplicate samples were processed at the SUNY upstate Microarray Core Facility. Gene expression levels were summarized by the GCRMA method (Wu et al., 2004). *P*-values were corrected for multiple comparisons using Benjamini-Hochberg's False Discovery Rate (FDR) method (Hochberg and Benjamini, 1990). Gene Ontology was performed with GO-Term Finder (http://amigo.geneontology.org/cgi-bin/amigo/term_enrichment) (Boyle et al., 2004). Data are available at the GEO repository (record number GSE58416).

Expression correlation in melanoma lines and tumors

Agilent microarrays were used. Data were processed by calculating parametric (Pearson) and nonparametric (Kendall) correlation in R, significance was evaluated with either Bonferroni corrections or by calculating the FDR using the 'phsych' package (Revelle, 2013). Two v-ATPase genes (ATP6V1C2 and ATP6V1G3) were excluded due to low expression. Four human MiT genes were assessed with one probe each. The average expression varied, the average TFEC A_24_P98210 expression was 78.6 (s.d.=25.1), TFE3 A_23_P84952 was 1284.1 (613.2), TFEB A_23_P368729 was 1415.7 (836.8) and MITF A_23_P61945 highest with 68613.2 (51574.2). We calculated the correlation of the four MiT factors and 23 v-ATPase genes, and tested whether the distribution of correlation coefficients differed from 0 with non-parametric Wilcoxon tests in R. The Pearson and Kendall correlation coefficients gave consistent results. Coupling of MITF-binding and v-ATPase gene expression was assessed by using a chi-squared and Fisher exact test in R. We similarly analyzed expression of MITF, other MiT genes and ATP6 loci in 331 melanoma tumors of the Cutaneous melanoma (SKCM) dataset available at The Cancer Genome Atlas (http://cancergenome.nih.gov). We calculated the Kendall correlation between gene pairs on RPKM expression estimates from data downloaded in February 2015.

M-Box analysis and ChIP

Bioinformatics programs used were MEME (http://meme-suite.org/tools/meme), Target Explorer (http://te.cryst.bbk.ac.uk) and VISTA (http://pipeline.lbl.gov/cgi-bin/gateway2?bg=dm2). Results were curated manually.

Late L3 *dpp-Gal4 UAS-MiTmyc 4Mbox-GFP* larvae were dissected and 150 pairs of wing discs and salivary glands were collected and fixed with 1% formaldehyde at 37°C for 15 min. After two washes with PBS (supplemented with protease inhibitors and PMSF), samples were lysed in 200 µl of lysis buffer (50 mM Tris-HCl pH 7.6, 1 mM $CaCl_2$, 0.2% NP-40, protease inhibitors and PMSF) by sonication. ChIP steps were as recommended in the ChIP assay kit (Upstate Biotechnology). PCR primers used are listed in supplementary material Table S8.

siRNA and qPCR of ATP6 genes in 501Mel cells

A previously described small interfering RNA (siRNA) against MITF [5′-r(AGCAGUACCUUUCUACCAC)d(TT)-3′] or a control sequence [5′-r(UUCUCC GAACGUGUCACGU)d(TT)-3′] were used (Carreira et al., 2006). Cells were transfected with 8.3 nM siRNA using Lipofectamine 2000 (Invitrogen) according to the manufacturer's protocol, and left for 72 h before harvesting for

analysis. Total RNA was extracted and cDNA synthesis performed using the RNeasy mini and QuantiTect Reverse Transcriptase Kits (QIAGEN). 50 ng cDNA was used for quantitative real-time PCR analysis (qPCR) on a Rotor Gene 6000 (QIAGEN) using the SensiMix SYBR Kit (Bioline). Reactions were carried out in technical and biological triplicates. Primer sequences are available on request.

Western blots

For *Drosophila*, 30 salivary gland pairs were dissected in cold PBS, transferred to 100 µl NP40 buffer on ice and prepared for SDS-PAGE. Primary antibodies were mouse anti-pS6K (1:1000; Cell Signaling, number 9206), guinea pig anti-S6K (1:3000; Hahn et al., 2010) and rabbit anti-GADPH (1:5000; Sigma G9545). Secondary antibodies were used at 1:5000. Detection used Clarity Western ECL Substrate (Bio-Rad), imaged on ChemiDoc Imaging System (Bio-Rad). For mammalian cell lines, 501Mel and SkMel28 cells with doxycycline-inducible MITF were generated using piggyback-transposon-based expression and kept under G418 selection in RPMI with 10% FBS (GIBCO). Cells were induced for 48 h (1 µg/ml doxycycline). Cell lysate in RIPA buffer were run on Tris-HEPES gels and blotted on 0.2 µM PVDF membranes. Primary antibodies were anti-β-actin (Cell Signaling Technology number 4970), anti-p70 S6 Kinase (Cell Signaling Technology number 2708), anti-phospho-p70 S6 Kinase (Thr389) (Cell Signaling Technology number 9206) and anti-MITF (Thermo number MS-771-PABX). Secondary antibodies were anti-mouse-IgG(H+L) DyLight 800 conjungate (Cell Signaling Technology number 5257) and a DyLight 680 conjungate anti-rabbit IgG (H+L) (CST #5366). Images were captured using Odyssey CLx Imager (LI-COR Biosciences). In both cases, quantification was by ImageJ.

Supplementary Material

Supplementary Material:

Acknowledgements

We thank Dr P. Kane and the Viczian, Zuber, Zhu and Pignoni laboratories for helpful discussions; C. Cara, R. Dilixiati, V. Thorsson, B.S. Haflidadottir for aid with cloning and bio informatics; Drs J. Dow, H. Kramer, G. Davis, E. Baehrecke, the BDSC and FlyTrap centers for fly stocks; the DSHB and Dr A. Teleman for antibodies; and the Molecular Analysis Core at SUNY-UMU for Affymetrix Gene Chip hybridization.

Footnotes

Competing interests

The authors declare no competing or financial interests.

Author contributions

F.P., T.Z., Q.Z., E.S., M.H.O., A.P., C.G., L.L. conceived and designed experiments and interpreted results. T.Z. and Q.Z. executed experiments in *Drosophila*; R.S., K.M. and L.L. executed experiments in melanoma cells. M.H., S.W.K., T.Z., F.P. analyzed microarray data. A.P., F.P., R.S. and E.S. performed evolutionary and bioinformatics analyses. F.P., E.S., T.Z., M.H.O., Q.Z. and A.P. wrote the manuscript.

Funding

This work was supported by the National Institutes of Health, National Eye Institute [grant number R01EY017097 to F.P.]; an RPB Unrestricted Grant and Lions District 20-Y1 award to the Dept. of Ophthalmology, SUNY-UMU (F.P.); the Icelandic Research Fund [grant numbers 130230-053 and 152715-051 to E.S.] a PHC Jules Verne 2014 grant [grant number 31891VM to E.S. and L.L.]; a grant from the Ligue Nationale Contre le Cancer (Equipe labellisee), INCa, Canceropole, Ile de France and Labex CelTisPhyBio [grant number ANR-11-LBX-0038 to L.L.]; and the Ludwig Institute for Cancer Research and the Harry J Lloyd Trust (to C.G.). Deposited in PMC for release after 12 months.

Supplementary material

Supplementary material available online at http://jcs.biologists.org/lookup/suppl/doi:10.1242/jcs.173807/-/DC1

References

Akbar M. A., Ray S. and Kramer H. (2009). The SM protein Car/Vps33A regulates SNARE-mediated trafficking to lysosomes and lysosome-related organelles. *Mol. Biol. Cell* 20, 1705-1714. 10.1091/mbc.E08-03-0282 [PMCID: PMC2655250] [PubMed: 19158398] [CrossRef: 10.1091/mbc.E08-03-0282]

Allan A. K., Du J., Davies S. A. and Dow J. A. T. (2005). Genome-wide survey of V-ATPase genes in Drosophila reveals a conserved renal phenotype for lethal alleles. *Physiol. Genomics* 22, 128-138. 10.1152/physiolgenomics.00233.2004 [PubMed: 15855386] [CrossRef: 10.1152/physiolgenomics.00233.2004]

Barolo S., Carver L. A. and Posakony J. W. (2000). GFP and beta-galactosidase transformation vectors for promoter/enhancer

analysis in Drosophila. *Biotechniques* 29, 726, 728, 730, 732. [PubMed: 11056799]

Blair H. C., Teitelbaum S. L., Ghiselli R. and Gluck S. (1989). Osteoclastic bone resorption by a polarized vacuolar proton pump. *Science* 245, 855-857. 10.1126/science.2528207 [PubMed: 2528207] [CrossRef: 10.1126/science.2528207]

Boyle E. I., Weng S., Gollub J., Jin H., Botstein D., Cherry J. M. and Sherlock G. (2004). GO::TermFinder--open source software for accessing Gene Ontology information and finding significantly enriched Gene Ontology terms associated with a list of genes. *Bioinformatics* 20, 3710-3715. 10.1093/bioinformatics/bth456 [PMCID: PMC3037731] [PubMed: 15297299] [CrossRef: 10.1093/bioinformatics/bth456]

Budd P. S. and Jackson I. J. (1995). Structure of the mouse tyrosinase-related protein-2/dopachrome tautomerase (Tyrp2/Dct) gene and sequence of two novel slaty alleles. *Genomics* 29, 35-43. 10.1006/geno.1995.1212 [PubMed: 8530099] [CrossRef: 10.1006/geno.1995.1212]

Burnett P. E., Barrow R. K., Cohen N. A., Snyder S. H. and Sabatini D. M. (1998). RAFT1 phosphorylation of the translational regulators p70 S6 kinase and 4E-BP1. *Proc. Natl. Acad. Sci. USA* 95, 1432-1437. 10.1073/pnas.95.4.1432 [PMCID: PMC19032] [PubMed: 9465032] [CrossRef: 10.1073/pnas.95.4.1432]

Carreira S., Goodall J., Denat L., Rodriguez M., Nuciforo P., Hoek K. S., Testori A., Larue L. and Goding C. R. (2006). Mitf regulation of Dia1 controls melanoma proliferation and invasiveness. *Genes Dev.* 20, 3426-3439. 10.1101/gad.406406 [PMCID: PMC1698449] [PubMed: 17182868] [CrossRef: 10.1101/gad.406406]

Chintapalli V. R., Wang J., Herzyk P., Davies S. A. and Dow J. A. T. (2013). Data-mining the FlyAtlas online resource to identify core functional motifs across transporting epithelia. *BMC Genomics* 14, 518 10.1186/1471-2164-14-518 [PMCID: PMC3734111] [PubMed: 23895496] [CrossRef: 10.1186/1471-2164-14-518]

Du J., Kean L., Allan A. K., Southall T. D., Davies S. A., McInerny C. J. and Dow J. A. T. (2006). The SzA mutations of the B subunit of the Drosophila vacuolar H+ ATPase identify conserved residues essential for function in fly and yeast. *J. Cell Sci.* 119, 2542-2551. 10.1242/jcs.02983 [PubMed: 16735441] [CrossRef: 10.1242/jcs.02983]

Hahn K., Miranda M., Francis V. A., Vendrell J., Zorzano A. and Teleman A. A. (2010). PP2A regulatory subunit PP2A-B′ counteracts S6K phosphorylation. *Cell Metab.* 11, 438-444. 10.1016/j.cmet.2010.03.015 [PubMed: 20444422] [CrossRef: 10.1016/j.cmet.2010.03.015]

Hallsson J. H., Haflidadóttir B. S., Stivers C., Odenwald W., Arnheiter H., Pignoni F. and Steingrímsson E. (2004). The basic helix-loop-helix leucine zipper transcription factor Mitf is conserved in Drosophila and functions in eye development. *Genetics* 167, 233-241. 10.1534/genetics.167.1.233 [PMCID: PMC1470875] [PubMed: 15166150] [CrossRef: 10.1534/genetics.167.1.233]

Hallsson J. H., Haflidadóttir B. S., Schepsky A., Arnheiter H. and Steingrímsson E. (2007). Evolutionary sequence comparison of the Mitf gene reveals novel conserved domains. *Pigment Cell Res.* 20, 185-200. 10.1111/j.1600-0749.2007.00373.x [PubMed: 17516926] [CrossRef: 10.1111/j.1600-0749.2007.00373.x]

Hermle T., Guida M. C., Beck S., Helmstädter S. and Simons M. (2013). Drosophila ATP6AP2/VhaPRR functions both as a novel planar cell polarity core protein and a regulator of endosomal trafficking. *EMBO J.* 32, 245-259. 10.1038/emboj.2012.323 [PMCID: PMC3553382] [PubMed: 23292348] [CrossRef: 10.1038/emboj.2012.323]

Hiesinger P. R., Fayyazuddin A., Mehta S. Q., Rosenmund T., Schulze K. L., Zhai R. G., Verstreken P., Cao Y., Zhou Y., Kunz J. et al. (2005). The v-ATPase V0 subunit a1 is required for a late step in synaptic vesicle exocytosis in Drosophila. *Cell* 121, 607-620. 10.1016/j.cell.2005.03.012 [PMCID: PMC3351201] [PubMed: 15907473] [CrossRef: 10.1016/j.cell.2005.03.012]

Hochberg Y. and Benjamini Y. (1990). More powerful procedures for multiple significance testing. *Stat. Med.* 9, 811-818. 10.1002/sim.4780090710 [PubMed: 2218183] [CrossRef: 10.1002/sim.4780090710]

Holland P. W., Garcia-Fernandez J., Williams N. A. and Sidow A. (1994). Gene duplications and the origins of vertebrate development. *Dev. Suppl.*, 125-133. [PubMed: 7579513]

Holliday S. L. (2014). Vacuolar H+-ATPase: an essential multitasking enzyme in physiology and pathophysiology. *New J. Sci.* 2014, 1-21. 10.1155/2014/675430 [CrossRef: 10.1155/2014/675430]

Isotani S., Hara K., Tokunaga C., Inoue H., Avruch J. and Yonezawa K. (1999). Immunopurified mammalian target of rapamycin phosphorylates and activates p70 S6 kinase alpha in vitro. *J. Biol. Chem.* 274, 34493-34498. 10.1074/jbc.274.48.34493 [PubMed: 10567431] [CrossRef: 10.1074/jbc.274.48.34493]

Iwaki D. D. and Lengyel J. A. (2002). A Delta–Notch signaling border regulated by Engrailed/Invected repression specifies boundary cells in the Drosophila hindgut. *Mech. Dev.* 114, 71-84. 10.1016/S0925-4773(02)00061-8 [PubMed: 12175491] [CrossRef: 10.1016/S0925-4773(02)00061-8]

Jones D. T., Taylor W. R. and Thornton J. M. (1992). The rapid generation of mutation data matrices from protein sequences. *Comput. Appl. Biosci.* 8, 275-282. 10.1093/bioinformatics/8.3.275 [PubMed: 1633570] [CrossRef: 10.1093/bioinformatics/8.3.275]

Juhasz G. and Neufeld T. P. (2008). Experimental control and characterization of autophagy in Drosophila. *Methods Mol. Biol.* 445, 125-133. 10.1007/978-1-59745-157-4_8 [PubMed: 18425447] [CrossRef: 10.1007/978-1-59745-157-4_8]

Kambadur R., Koizumi K., Stivers C., Nagle J., Poole S. J. and Odenwald W. F. (1998). Regulation of POU genes by castor and hunchback establishes layered compartments in the Drosophila CNS. *Genes Dev.* 12, 246-260. 10.1101/gad.12.2.246 [PMCID: PMC316437] [PubMed: 9436984] [CrossRef: 10.1101/gad.12.2.246]

Lee B. S. (2012). Regulation of V-ATPase expression in mammalian cells. *Curr. Protein Pept. Sci.* 13, 107-116. 10.2174/138920312800493188 [PubMed: 22044154] [CrossRef: 10.2174/138920312800493188]

Lee Y. S. and Carthew R. W. (2003). Making a better RNAi vector for Drosophila: use of intron spacers. *Methods* 30, 322-329. 10.1016/S1046-2023(03)00051-3 [PubMed: 12828946] [CrossRef: 10.1016/S1046-2023(03)00051-3]

Marois E., Mahmoud A. and Eaton S. (2006). The endocytic pathway and formation of the Wingless morphogen gradient. *Development* 133, 307-317. 10.1242/dev.02197 [PubMed: 16354714] [CrossRef: 10.1242/dev.02197]

Marshansky V., Rubinstein J. L. and Grüber G. (2014). Eukaryotic V-ATPase: novel structural fingdings and finctional insights. *Biochim. Biophys. Acta.* 1837, 857-879. 10.1016/j.bbabio.2014.01.018 [PubMed: 24508215] [CrossRef: 10.1016/j.bbabio.2014.01.018]

Martina J. A. and Puertollano R. (2013). Rag GTPases mediate amino acid-dependent recruitment of TFEB and MITF to lysosomes. *J. Cell Biol.* 200, 475-491. 10.1083/jcb.201209135 [PMCID: PMC3575543] [PubMed: 23401004] [CrossRef: 10.1083/jcb.201209135]

Martina J. A., Chen Y., Gucek M. and Puertollano R. (2012). MTORC1 functions as a transcriptional regulator of autophagy by preventing nuclear transport of TFEB. *Autophagy* 8, 903-914. 10.4161/auto.19653 [PMCID: PMC3427256] [PubMed: 22576015] [CrossRef: 10.4161/auto.19653]

Martina J. A., Diab H. I., Li H. and Puertollano R. (2014). Novel roles for the MiTF/TFE family of transcription factors in organelle biogenesis, nutrient sensing, and energy homeostasis. *Cell Mol. Life Sci.* 71, 2483-2497. 10.1007/s00018-014-1565-8 [PMCID: PMC4057939] [PubMed: 24477476] [CrossRef: 10.1007/s00018-014-1565-8]

Mauvezin C., Ayala C., Braden C. R., Kim J. and Neufeld T. P. (2014). Assays to monitor autophagy in Drosophila. *Methods* 68, 134-139. 10.1016/j.ymeth.2014.03.014 [PMCID: PMC4048785] [PubMed: 24667416] [CrossRef: 10.1016/j.ymeth.2014.03.014]

Mindell J. A. (2012). Lysosomal acidification mechanisms. *Annu. Rev. Physiol.* 74, 69-86. 10.1146/annurev-physiol-012110-142317 [PubMed: 22335796] [CrossRef: 10.1146/annurev-physiol-012110-142317]

Morii E., Takebayashi K., Motohashi H., Yamamoto M., Nomura S. and Kitamura Y. (1994). Loss of DNA binding ability of the transcription factor encoded by the mutant mi locus. *Biochem. Biophys. Res. Commun.* 205, 1299-1304. 10.1006/bbrc.1994.2806 [PubMed: 7802662] [CrossRef: 10.1006/bbrc.1994.2806]

Nelson N., Perzov N., Cohen A., Hagai K., Padler V. and Nelson H. (2000). The cellular biology of proton-motive force generation by V-ATPases. *J. Exp. Biol.* 203, 89-95. [PubMed: 10600677]

Nishisho T., Hata K., Nakanishi M., Morita Y., Sun-Wada G.-H., Wada Y., Yasui N. and Yoneda T. (2011). The a3 isoform vacuolar

type H+-ATPase promotes distant metastasis in the mouse B16 melanoma cells. *Mol. Cancer Res.* 9, 845-855. 10.1158/1541-7786.MCR-10-0449 [PubMed: 21669964] [CrossRef: 10.1158/1541-7786.MCR-10-0449]

Ohno S. (1999). Gene duplication and the uniqueness of vertebrate genomes circa 1970–1999. *Semin. Cell Dev. Biol.* 10, 517-522. 10.1006/scdb.1999.0332 [PubMed: 10597635] [CrossRef: 10.1006/scdb.1999.0332]

Palmieri M., Impey S., Kang H., di Ronza A., Pelz C., Sardiello M. and Ballabio A. (2011). Characterization of the CLEAR network reveals an integrated control of cellular clearance pathways. *Hum. Mol. Genet.* 20, 3852-3866. 10.1093/hmg/ddr306 [PubMed: 21752829] [CrossRef: 10.1093/hmg/ddr306]

Peña-Llopis S. and Brugarolas J. (2011). TFEB, a novel mTORC1 effector implicated in lysosome biogenesis, endocytosis and autophagy. *Cell Cycle* 10, 3987-3988. 10.4161/cc.10.23.18251 [PMCID: PMC3272281] [PubMed: 22101272] [CrossRef: 10.4161/cc.10.23.18251]

Peña-Llopis S., Vega-Rubin-de-Celis S., Schwartz J. C., Wolff N. C., Tran T. A. T., Zou L., Xie X.-J., Corey D. R. and Brugarolas J. (2011). Regulation of TFEB and V-ATPases by mTORC1. *EMBO J.* 30, 3242-3258. 10.1038/emboj.2011.257 [PMCID: PMC3160667] [PubMed: 21804531] [CrossRef: 10.1038/emboj.2011.257]

Pulipparacharuvil S., Akbar M. A., Ray S., Sevrioukov E. A., Haberman A. S., Rohrer J. and Krämer H. (2005). Drosophila Vps16A is required for trafficking to lysosomes and biogenesis of pigment granules. *J. Cell Sci.* 118, 3663-3673. 10.1242/jcs.02502 [PubMed: 16046475] [CrossRef: 10.1242/jcs.02502]

Revelle W. (2013). *psych: Procedures for Personality and Psychological Research*. Evanston, Illinois, USA: Northwestern University.

Roczniak-Ferguson A., Petit C. S., Froehlich F., Qian S., Ky J., Angarola B., Walther T. C. and Ferguson S. M. (2012). The transcription factor TFEB links mTORC1 signaling to transcriptional control of lysosome homeostasis. *Sci. Signal.* 5, ra42 10.1126/scisignal.2002790 [PMCID: PMC3437338] [PubMed: 22692423] [CrossRef: 10.1126/scisignal.2002790]

Sardiello M., Palmieri M., di Ronza A., Medina D. L., Valenza M., Gennarino V. A., Di Malta C., Donaudy F., Embrione V., Polishchuk R. S. et al. (2009). A gene network regulating lysosomal biogenesis and function. *Science* 325, 473-477. 10.1126/science.1174447 [PubMed: 19556463] [CrossRef: 10.1126/science.1174447]

Scimeca J.-C., Franchi A., Trojani C., Parrinello H., Grosgeorge J., Robert C., Jaillon O., Poirier C., Gaudray P. and Carle G. F. (2000). The gene encoding the mouse homologue of the human osteoclast-specific 116-kDa V-ATPase subunit bears a deletion in osteosclerotic (oc/oc) mutants. *Bone* 26, 207-213. 10.1016/S8756-3282(99)00278-1 [PubMed: 10709991] [CrossRef: 10.1016/S8756-3282(99)00278-1]

Settembre C., Di Malta C., Polito V. A., Garcia Arencibia M., Vetrini F., Erdin S., Erdin S. U., Huynh T., Medina D., Colella P. et al.

(2011). TFEB links autophagy to lysosomal biogenesis. *Science* 332, 1429-1433. 10.1126/science.1204592 [PMCID: PMC3638014] [PubMed: 21617040] [CrossRef: 10.1126/science.1204592]

Settembre C., Zoncu R., Medina D. L., Vetrini F., Erdin S., Erdin S., Huynh T., Ferron M., Karsenty G., Vellard M. C. et al. (2012). A lysosome-to-nucleus signalling mechanism senses and regulates the lysosome via mTOR and TFEB. *EMBO J.* 31, 1095-1108. 10.1038/emboj.2012.32 [PMCID: PMC3298007] [PubMed: 22343943] [CrossRef: 10.1038/emboj.2012.32]

Sievers F. and Higgins D. G. (2014). Clustal Omega, accurate alignment of very large numbers of sequences. *Methods Mol. Biol.* 1079, 105-116. 10.1007/978-1-62703-646-7_6 [PubMed: 24170397] [CrossRef: 10.1007/978-1-62703-646-7_6]

Steingrimsson E., Tessarollo L., Pathak B., Hou L., Arnheiter H., Copeland N. G. and Jenkins N. A. (2002). Mitf and Tfe3, two members of the Mitf-Tfe family of bHLH-Zip transcription factors, have important but functionally redundant roles in osteoclast development. *Proc. Natl. Acad. Sci. USA* 99, 4477-4482. 10.1073/pnas.072071099 [PMCID: PMC123673] [PubMed: 11930005] [CrossRef: 10.1073/pnas.072071099]

Steingrímsson E., Copeland N. G. and Jenkins N. A. (2004). Melanocytes and the microphthalmia transcription factor network. *Annu. Rev. Genet.* 38, 365-411. 10.1146/annurev.genet.38.072902.092717 [PubMed: 15568981] [CrossRef: 10.1146/annurev.genet.38.072902.092717]

Strub T., Giuliano S., Ye T., Bonet C., Keime C., Kobi D., Le Gras S., Cormont M., Ballotti R., Bertolotto C. et al. (2011). Essential role of microphthalmia transcription factor for DNA replication, mitosis and genomic stability in melanoma. *Oncogene* 30, 2319-2332. 10.1038/onc.2010.612 [PubMed: 21258399] [CrossRef: 10.1038/onc.2010.612]

Sweeney S. T. and Davis G. W. (2002). Unrestricted synaptic growth in spinster—a late endosomal protein implicated in TGF-beta-mediated synaptic growth regulation. *Neuron* 36, 403-416. 10.1016/S0896-6273(02)01014-0 [PubMed: 12408844] [CrossRef: 10.1016/S0896-6273(02)01014-0]

Tamura K., Stecher G., Peterson D., Filipski A. and Kumar S. (2013). MEGA6: Molecular Evolutionary Genetics Analysis version 6.0. *Mol. Biol. Evol.* 30, 2725-2729. 10.1093/molbev/mst197 [PMCID: PMC3840312] [PubMed: 24132122] [CrossRef: 10.1093/molbev/mst197]

Thummel C. S. and Pirrotta V. (1991). Technical notes: new pCaSpeR P-element vectors. *Drosophila Info. Newsl.* 2.

Toei M., Saum R., Forgac M. (2010). Regulation and isoform function of the V-ATPases. *Biochemistry* 49, 4715-23. 10.1021/bi100397s [PMCID: PMC2907102] [PubMed: 20450191] [CrossRef: 10.1021/bi100397s]

Udagawa N., Sasaki T., Akatsu T., Takahashi N., Tanaka S., Tamura T., Tanaka H. and Suda T. (1992). Lack of bone resorption in osteosclerotic (oc/oc) mice is due to a defect in osteoclast progenitors rather than the local microenvironment provided by

osteoblastic cells. *Biochem. Biophys. Res. Commun.* 184, 67-72. 10.1016/0006-291X(92)91158-M [PubMed: 1567458] [CrossRef: 10.1016/0006-291X(92)91158-M]

Vaccari T., Duchi S., Cortese K., Tacchetti C. and Bilder D. (2010). The vacuolar ATPase is required for physiological as well as pathological activation of the Notch receptor. *Development* 137, 1825-1832. 10.1242/dev.045484 [PMCID: PMC2867318] [PubMed: 20460366] [CrossRef: 10.1242/dev.045484]

Waterhouse R. M., Tegenfeldt F., Li J., Zdobnov E. M. and Kriventseva E. V. (2013). OrthoDB: a hierarchical catalog of animal, fungal and bacterial orthologs. *Nucleic Acids Res.* 41, D358-D365. 10.1093/nar/gks1116 [PMCID: PMC3531149] [PubMed: 23180791] [CrossRef: 10.1093/nar/gks1116]

Webster D. E., Barajas B., Bussat R. T., Yan K. J., Neela P. H., Flockhart R. J., Kovalski J., Zehnder A. and Khavari P. A. (2014). Enhancer-targeted genome editing selectively blocks innate resistance to oncokinase inhibition. *Genome Res.* 24, 751-760. 10.1101/gr.166231.113 [PMCID: PMC4009605] [PubMed: 24443471] [CrossRef: 10.1101/gr.166231.113]

Wieczorek H., Beyenbach K. W., Huss M. and Vitavska O. (2009). Vacuolar-type proton pumps in insect epithelia. *J. Exp. Biol.* 212, 1611-1619. 10.1242/jeb.030007 [PMCID: PMC2683008] [PubMed: 19448071] [CrossRef: 10.1242/jeb.030007]

Wu Z., Irizarry R. A., Gentleman R., Martinez-Murillo F. and Spencer F. (2004). A model-based background adjustment for oligonucleotide expression arrays. *J. Am. Stat. Assoc.* 99, 909-917. 10.1198/016214504000000683 [CrossRef: 10.1198/016214504000000683]

Yan Y., Denef N. and Schüpbach T. (2009). The vacuolar proton pump, V-ATPase, is required for notch signaling and endosomal trafficking in Drosophila. *Dev. Cell* 17, 387-402. 10.1016/j.devcel.2009.07.001 [PMCID: PMC2758249] [PubMed: 19758563] [CrossRef: 10.1016/j.devcel.2009.07.001]

Yu L., McPhee C. K., Zheng L., Mardones G. A., Rong Y., Peng J., Mi N., Zhao Y., Liu Z., Wan F. et al. (2010). Termination of autophagy and reformation of lysosomes regulated by mTOR. *Nature* 465, 942-946. 10.1038/nature09076 [PMCID: PMC2920749] [PubMed: 20526321] [CrossRef: 10.1038/nature09076]

Yu L., Zhou Q. and Pignoni F. (2015). ato-Gal4 fly lines for gene function analysis: eya is required in late progenitors for eye morphogenesis. *Genesis* 53, 347-355. 10.1002/dvg.22858 [PMCID: PMC5063080] [PubMed: 25980363] [CrossRef: 10.1002/dvg.22858]

Zoncu R., Bar-Peled L., Efeyan A., Wang S., Sancak Y. and Sabatini D. M. (2011). mTORC1 senses lysosomal amino acids through an inside-out mechanism that requires the vacuolar H+-ATPase. *Science* 334, 678-683. 10.1126/science.1207056 [PMCID: PMC3211112] [PubMed: 22053050] [CrossRef: 10.1126/science.1207056]

Figures and Tables

Fig. 1.

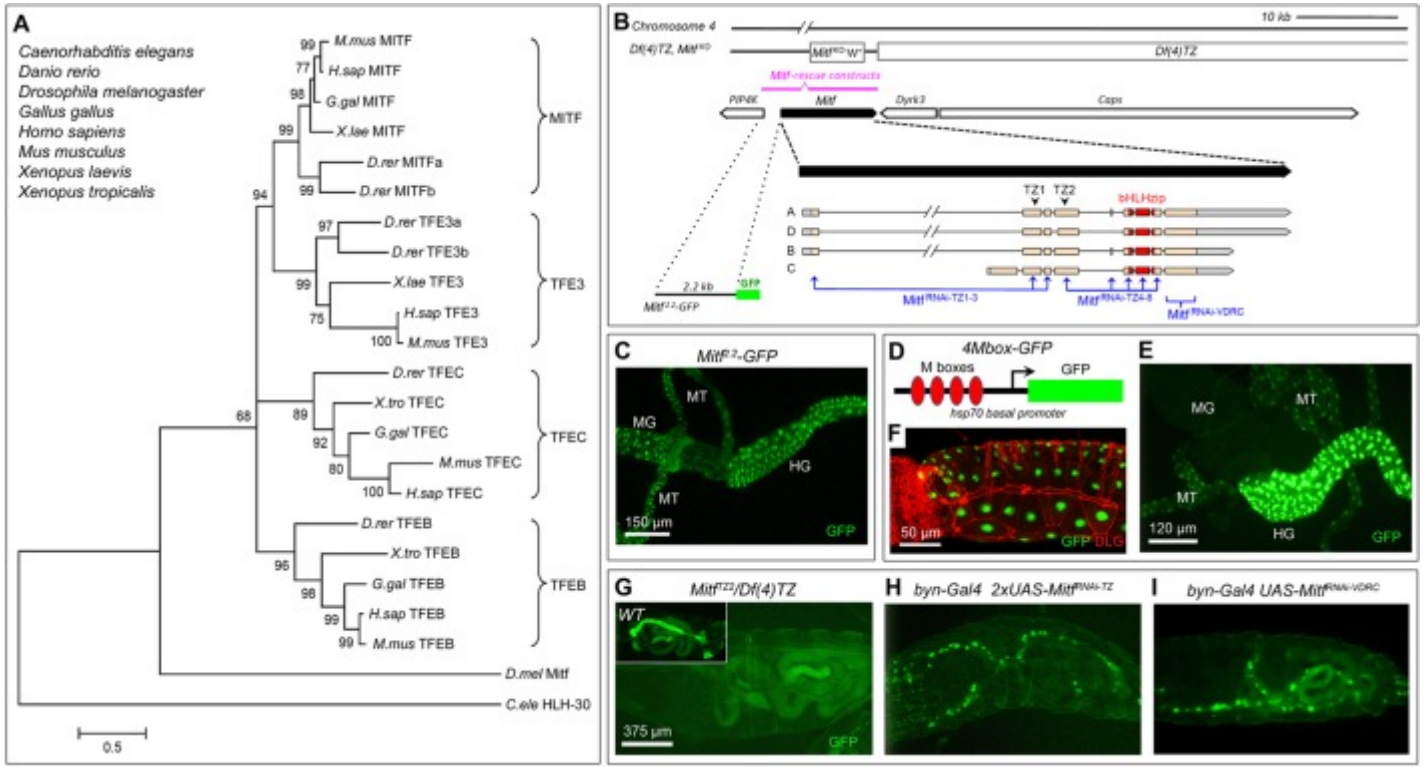

***Mitf* is evolutionarily conserved and functions in gut.** (A) Evolutionary conservation of fly and vertebrate MiT factors as assessed using the Maximum Likelihood method. The tree is to scale with branch lengths measured in number of changes per site (0.5). Monophyletic groups representing orthologous gene families are shown with brackets on the right. MITF and TFE3 clustering is strongly supported. Extra whole genome duplications occurred in the fish branch, generating duplicate copies in *D. rerio*. (B) *Mitf* gene and reagents. The genes *PIP4K*, *Dyrk3*, and *Caps* and four Mitf mRNA isoforms are shown (Flybase). The bHLHZip region is marked in red. Double slashes (//) in the *Mitf* intron 1 reflect a ~20 kb genomic region with repeated DNA. $Df(4)TZ^{DC}$, $Mitf^{KO}$ [=*Df(4)TZ*] removes *Mitf*, *Dyrk3* and *Caps*. Mitf rescue constructs span the *Mitf* DNA except for part of intron 1 (magenta). Arrowheads show sites of $Mitf^{TZ1}$ and $Mitf^{TZ2}$ nonsense mutations. dsRNA transgenes $Mitf^{RNAi\text{-}TZ1\text{-}3}$, $Mitf^{RNAi\text{-}TZ4\text{-}8}$ and $Mitf^{RNAi\text{-}VDRC}$ (KK113614)

target exons shown by linked arrows or bracket in blue. The *Mitf*$^{2.2}$*-GFP* reporter contains 2.2 kb of upstream DNA and 5′UTR driving nuclear GFP. (C–I) Gut and/or Malpighian tubules of L1–L3 larvae; anterior to the left; all panels show nuclear GFP (green; anti-GFP antibody); in panel F, Dlg (red; anti-Dlg antibody) marks cell membranes. (C) *Mitf*$^{2.2}$*-GFP* expression in wild-type (WT) L3 midgut (MG), hindgut (HG) and Malpighian tubules (MT). (D–I) *4Mbox-GFP* expression in wild type (E,F) and mutants (G–I). (D) Diagram of *4Mbox-GFP*. (E) *4Mbox-GFP* expression is present in L3 hindgut and Malpighian tubules, but not midgut. (F) Higher magnification of *4Mbox-GFP* in hindgut shows expression in cells of the gut lining. (G–I) *4Mbox-GFP* expression is Mitf dependent. All panels show live larvae; anterior to the left. (G) *4Mbox-GFP* expression is reduced in midgut, hindgut and Malpighian tubules of L1 *Mitf*^{TZ2}*/Df(4)TZ*; residual weak expression is likely due to stop-codon read-through or residual maternal product. Inset shows expression in wild type. (H,I) In *byn-Gal4 UAS-Mitf*^{RNAi} L2 larvae, *4Mbox-GFP* expression is lost in the hindgut but not Malpighian tubules, as expected for *byn-Gal4*; (H) *byn-Gal4 UAS-Mitf*$^{RNAi\text{-}TZ1\text{-}3}$ *UAS-Mitf*$^{RNAi\text{-}TZ4\text{-}8}$; (I) *byn-Gal4 UAS-Mitf*$^{RNAi\text{-}VDRC}$.

Fig. 2.

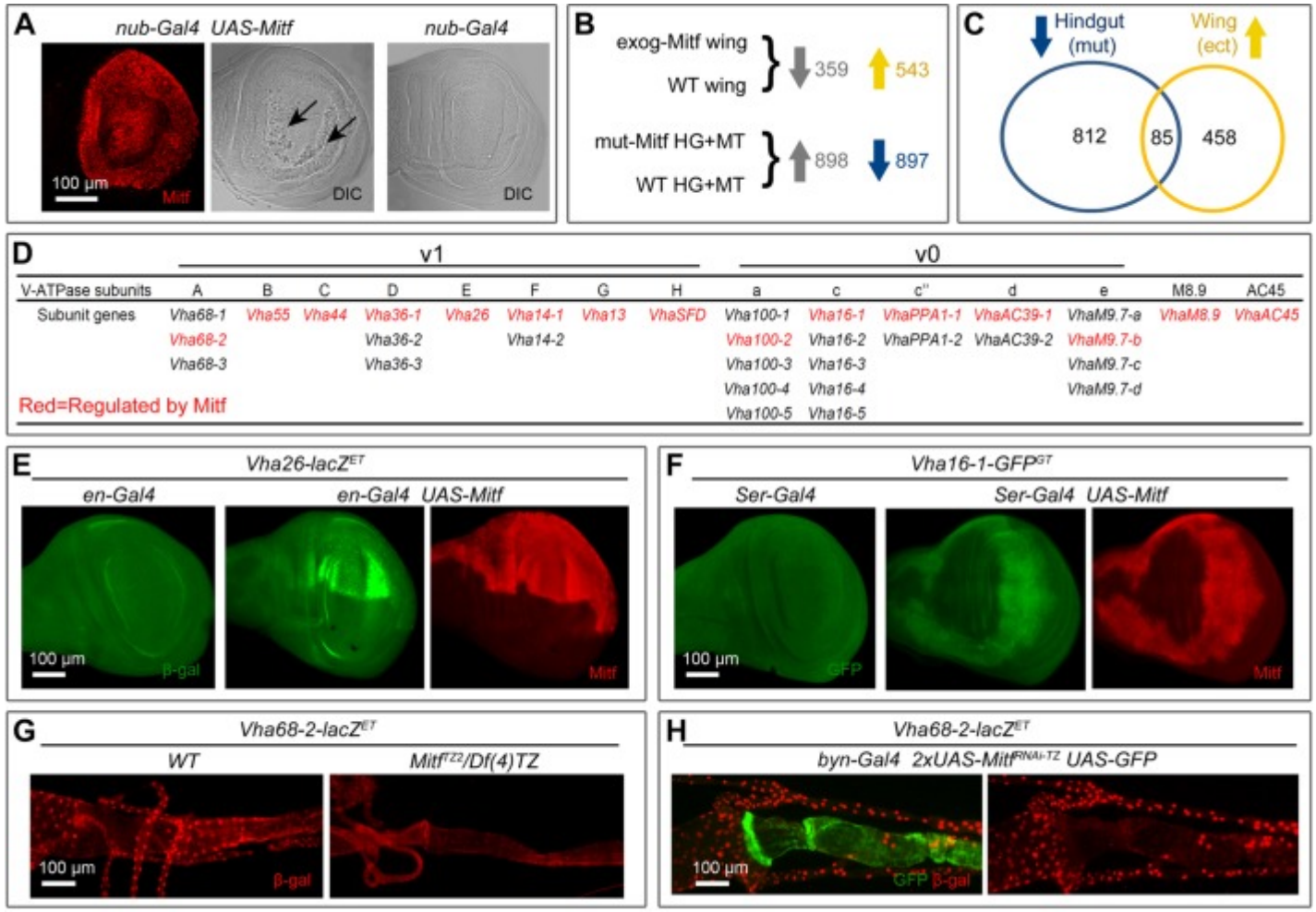

Mitf controls expression of v-ATPase subunit genes. Summary and validation of microarray analysis. (A) *nub-Gal4 UAS-Mitf* L3 wing discs expressing exogenous Mitf in the wing pouch (red; anti-Mitf antibody). DIC of same disc showing aberrant morphology and cell death (arrows), and a

control *nub-Gal4* disc. (B) As compared to wild-type (WT) tissues, 543 genes were upregulated and 359 genes were downregulated (≥1.4 fold; $P \leq 0.01$) by exogenous (exog) Mitf in wing discs; whereas 897 genes were downregulated and 898 upregulated (≥1.4 fold; *P* value ≤0.01) in mutant (mut) hindgut (HG)+Malpighian tubules (MT). (C) 85 genes were upregulated in wing (by ectopic expression, ect) and downregulated in mutant hindgut+Malpighian tubules. (D) 33 *Vha* genes encode the 15 subunits of the v-ATPase (known as V1A–V1H for the V1 complex and V0a–V0e for the V0 complex; M8.9 and AC45 are accessory subunits called AP1 and AP2 in mammals). Mitf controls the 15 *Vha* genes shown in red; one for each component of the holoenzyme. (E,F) Validation of microarray findings in wing discs. (E) *en-Gal4 Vha26-lacZ*^{ET} and *en-Gal4 UAS-Mitf Vha26-lacZ*^{ET} wing discs showing upregulation of *Vha26-lacZ*^{ET} expression (green; anti-β-Gal antibody) where Mitf protein is present (red; anti-Mitf antibody). (F) *Ser-Gal4 Vha16-1-GFP*^{GT} and *Ser-Gal4 UAS-Mitf Vha16-1-GFP*^{GT} wing discs showing upregulation of *Vha16-1-GFP*^{GT} (green; anti-GFP antibody) where Mitf protein is present (red; anti-Mitf antibody). (G,H) Downregulation of *Vha* genes in mutant and RNAi larvae. (G) *Vha68-2-lacZ*^{ET} and *Vha68-2-lacZ*^{ET} *Mitf*^{TZ2}/*Df(4)TZ* larval hindgut and Malpighian tubules show downregulation of enhancer trap expression (red; anti-β-Gal antibody) when *Mitf* is reduced. (H) In *byn-Gal4 UAS-GFP 2xUAS-Mitf*$^{RNAi\text{-}TZ}$ *Vha68-2-lacZ*^{ET} L3 larvae, GFP expression (green; anti-GFP antibody) marks hindgut cells with RNAi co-expression (left panel); enhancer trap *Vha68-2-lacZ*^{ET} expression (red; anti-β-Gal antibody) is absent in the hindgut, but present in midgut and Malpighian tubules (right panel).

Fig. 3.

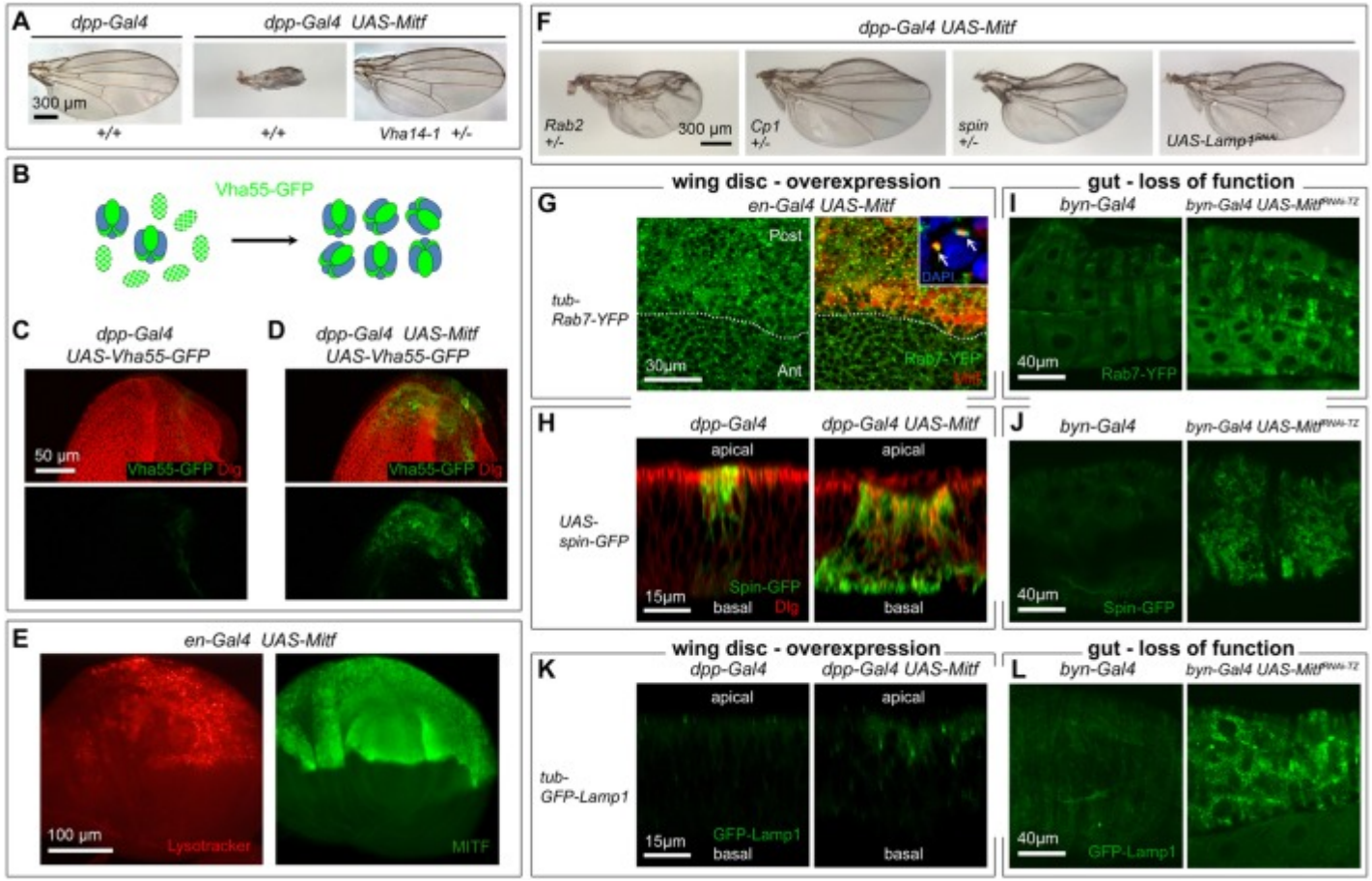

Exogenous Mitf affects holoenzyme activity and lysosomal pathway *in vivo*. Genotypes are as marked around panels. (A) *Vha* loss-of-function alleles dominantly suppress (right) wing defects caused by Mitf overexpression (middle). (B–D) Vha55–GFP expression increases in the presence of Mitf protein. (B) Diagram showing that the stability of the Vha55–GFP fusion protein correlates with the amount of assembled v-ATPase. (C,D) Panels show the dorsal region of *dpp-Gal4 UAS-Vha55-GFP* eye discs where *dpp-Gal4* drives robust expression. Discs are stained for GFP (green; anti-GFP

antibody) and the cell membrane marker Dlg (red; anti-Dlg antibody). The fusion protein is detected in the presence (D) but not in the absence (C) of Mitf. (E) Strong Lysotracker staining (red) is present in the posterior half (top) of the *en-Gal4 UAS-Mitf* wing disc, where Mitf is expressed (green; anti-Mitf antibody). (F) Reduction of lysosomal factors suppresses Mitf-induced wing defects. (G,H) Effect of Mitf overexpression on lysosomal vesicles in the wing. (G) Disc expressing Rab7–YFP ubiquitously but Mitf only in the posterior region shows increased Rab7–YFP (green; anti-GFP antibody) where Mitf is present (red; anti-Mitf antibody). Inset shows Mitf- and Rab7-positive punctae near the nucleus (DAPI) of a posterior wing-disc cell. (H) Confocal Z-sections along midline of *dpp-gal4 UAS-spin-GFP* wing discs without (left) or with (right) *UAS-Mitf*. Spin-GFP expression (green; anti-GFP antibody) expands (cell membranes in red; anti-Dlg antibody) in the presence of exogenous Mitf (not stained in this disc). (I,J) Effect of Mitf loss on lysosomal vesicles in the gut. Overall Rab7–YFP (I) or Spin–GFP (J) staining (green; anti-GFP antibody) increases in the hindgut from *byn-Gal4 UAS-Mitf*$^{RNAi\text{-}TZ}$ L3 larvae. Punctate staining is also visibly increased as compared to *byn-Gal4* controls. (K,L) *In vivo* assessment of lysosomal function using the lysosomal activity sensor *tub-GFP-Lamp1* (green; anti-GFP antibody) in gain-of-Mitf wing disc (K) and loss-of-Mitf hindgut (L). (K) Mitf overexpression (right) increases the level of GFP only slightly over Gal4-only control (left), indicating efficient GFP degradation. (L) Loss-of-Mitf dramatically increases GFP expression (right) as compared to control (left), indicating a failure of protein degradation.

Fig. 4.

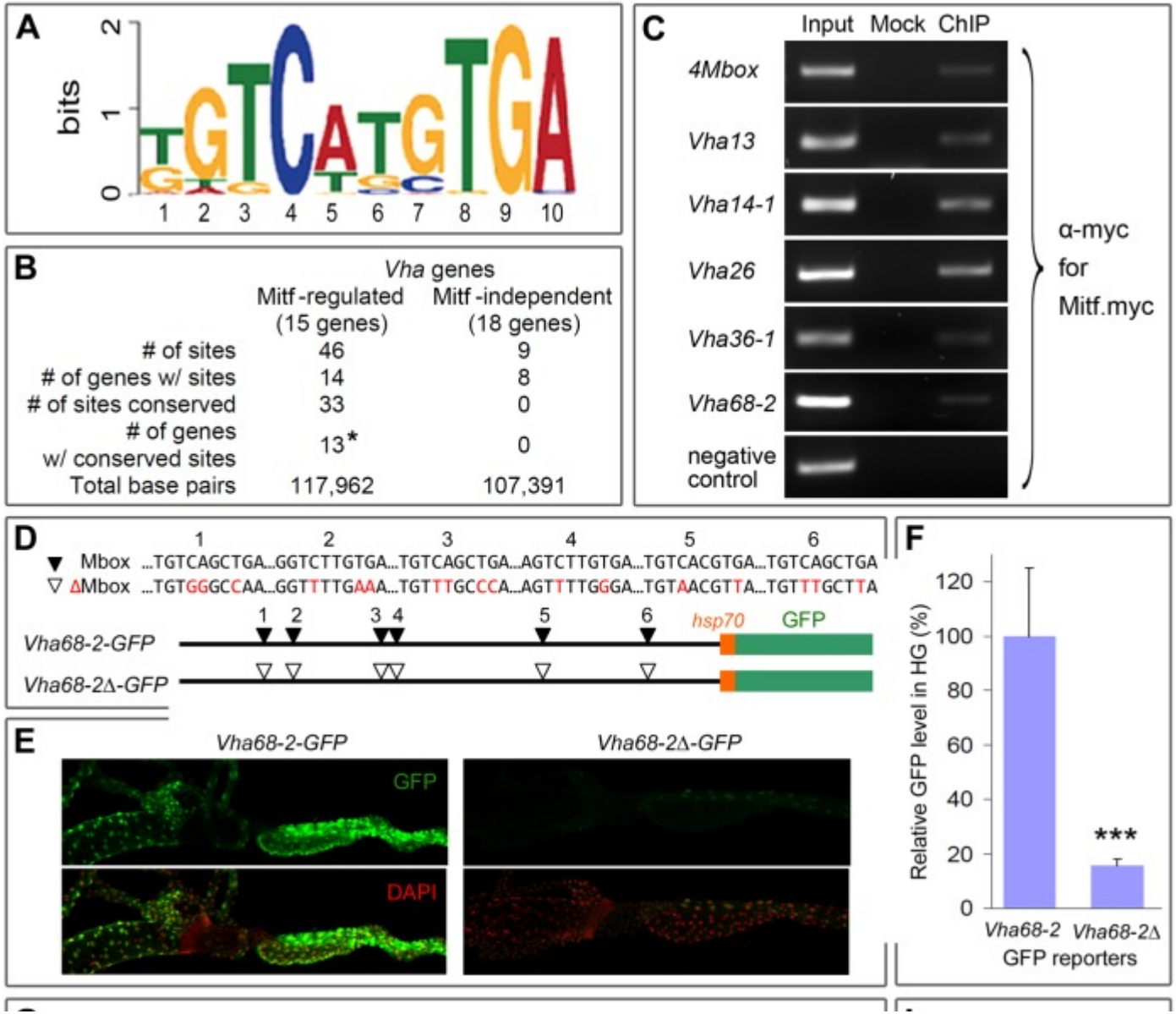
A
bits
2
1
0
1 2 3 4 5 6 7 8 9 10
B
Vha genes
Mitf-regulated (15 genes)
Mitf-independent (18 genes)
# of sites 46 9
# of genes w/ sites 14 8
# of sites conserved 33 0
# of genes w/ conserved sites 13* 0
Total base pairs 117,962 107,391
C
Input Mock ChIP
4Mbox
Vha13
Vha14-1
Vha26
Vha36-1
Vha68-2
negative control
α-myc for Mitf.myc
D
1 2 3 4 5 6
Mbox ...TGTCAGCTGA...GGTCTTGTGA...TGTCAGCTGA...AGTCTTGTGA...TGTCACGTGA...TGTCAGCTGA
ΔMbox ...TGTGGGCCAA...GGTTTTGAAA...TGTTTGCCCA...AGTTTTGGGA...TGTAACGTTA...TGTTTGCTTA
hsp70
GFP
Vha68-2-GFP
Vha68-2Δ-GFP
E
Vha68-2-GFP
Vha68-2Δ-GFP
GFP
DAPI
F
Relative GFP level in HG (%)
120
100
80
60
40
20
0
***
Vha68-2
Vha68-2Δ
GFP reporters

Open in a separate window

Mitf directly regulates *Vha* gene expression in the fly. Mitf-binding site identification and testing. (A) Consensus sequence of the 10-bp M-box binding site enriched in 15 Mitf-regulated *Vha* genes. (B) Evolutionarily conserved sites are found in 13 Mitf-dependent *Vha* genes, but are absent from 18 non-regulated *Vha* loci. The remaining two Mitf-regulated loci (not included in *) contain evolutionarily conserved M-box sequences matching the 8-bp core consensus. (C) ChIP confirms binding of Mitf–Myc protein to M-box-containing *Vha* regulatory regions (from wing discs and salivary glands cells expressing exogenous Mitf–Myc). (D–I) Analysis of *Vha-GFP* reporters containing wild-type or M-box-mutated regulatory genomic DNA. (D,G) Diagrams of the reporters *Vha68-2-GFP* (D) and *Vha13-GFP* (G), including M-box sequences and mutated base pairs (red). Upside-down triangles mark the positions of the sites. The *hsp70* basal promoter (orange box) was used for the *Vha68-2* intronic regulatory region; whereas the endogenous promoter with the 5′-flanking genomic fragment was sufficient for *Vha13*. (E,H) For both *Vha68-2* and *Vha13* reporters, GFP (nuclear) expression is strongly induced by endogenous Mitf in midgut, hindgut and Malpighian tubules, but is severely reduced when the sites are mutated. (F,I) Quantification of GFP expression levels for wild-type and mutant *Vha68-2* (F) and *Vha13* (I) reporters. ***$P<0.0001$ (one-tailed Student's *t*-test).

Fig. 5.

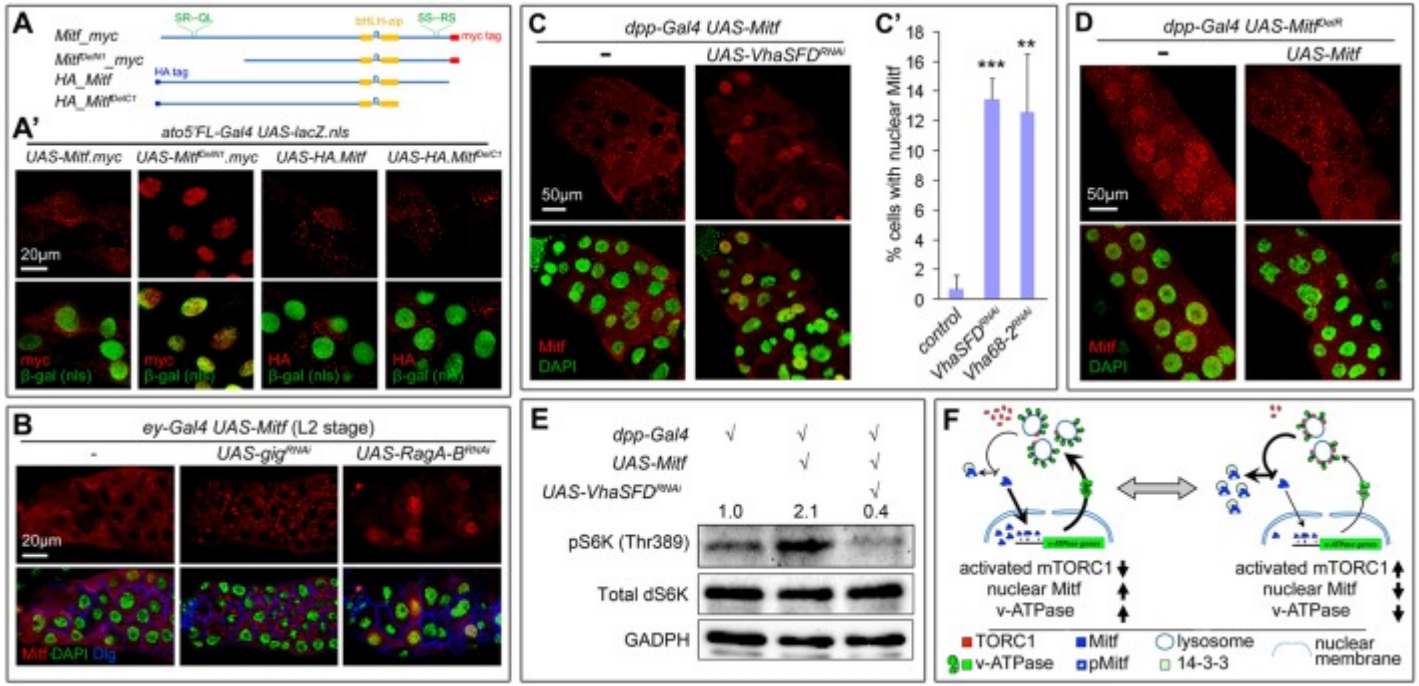

Mitf, v-ATPase and TORC1 form a homeostatic feedback loop. (A) Diagram of wild-type and truncated proteins lacking the Rag-binding or the S-rich regions. (A′) Panels show staining for Mitf proteins (red; anti-Myc or anti-HA antibody) and nuclear β-galactosidase (green; anti-β-Gal antibody). Genotypes are as marked above. Notice that the full length and the truncated Mitf^{DelC1} proteins are cytoplasmic, whereas the truncated Mitf^{DelN1} protein is nuclear. (B) Exogenous Mitf protein driven by *ey-Gal4* in salivary gland cells is detected mainly in the cytoplasm. RNAi-mediated knockdown of the negative TORC1 regulator *gig* enhances the cytoplasmic, punctate expression of Mitf. Conversely, knockdown of the positive TORC1 regulator *RagA-B* shifts Mitf localization to the nucleus. See supplementary material Fig. S3A,A′ for quantification. (C,C′) Knockdown of *VhaSFD* (or *Vha68-2*; not shown) shifts wild-type Mitf protein localization from the cytoplasm (left panels) to the nucleus (right panels). Quantification of nuclear localization is shown in C′ as a percentage of total cells scored (Y-axis). ***P*<0.01; ****P*<0.0001 (one-tailed Student's *t*-test). (D) Exogenous, nonfunctional Mitf^{DelR} mutant protein is distributed throughout the nucleus and cytoplasm in salivary gland cells (left panels); co-expression of wild-type Mitf shifts the balance

of protein localization to the cytoplasm (right panels). (E) Western blot shows that the level of pS6K increases in the presence of exogenous Mitf, but decreases if the level of a v-ATPase component is reduced (UAS-*VhaSFD*^{RNAi}). Numbers show the relative band intensity compared to a Gal4-only control set as 1; a similar blot showed a 1:2.3:0.5 ratio (not shown). Total *Drosophila* (d)S6K does not change significantly; GADPH was used as loading control. (F) The diagram shows the consequences of the regulatory relationship among loop components. The Mitf/v-ATPase/TORC1 regulatory loop maintains the activity levels of these important metabolic regulators within an optimal range in response to intrinsic and environmental influences.

Fig. 6.

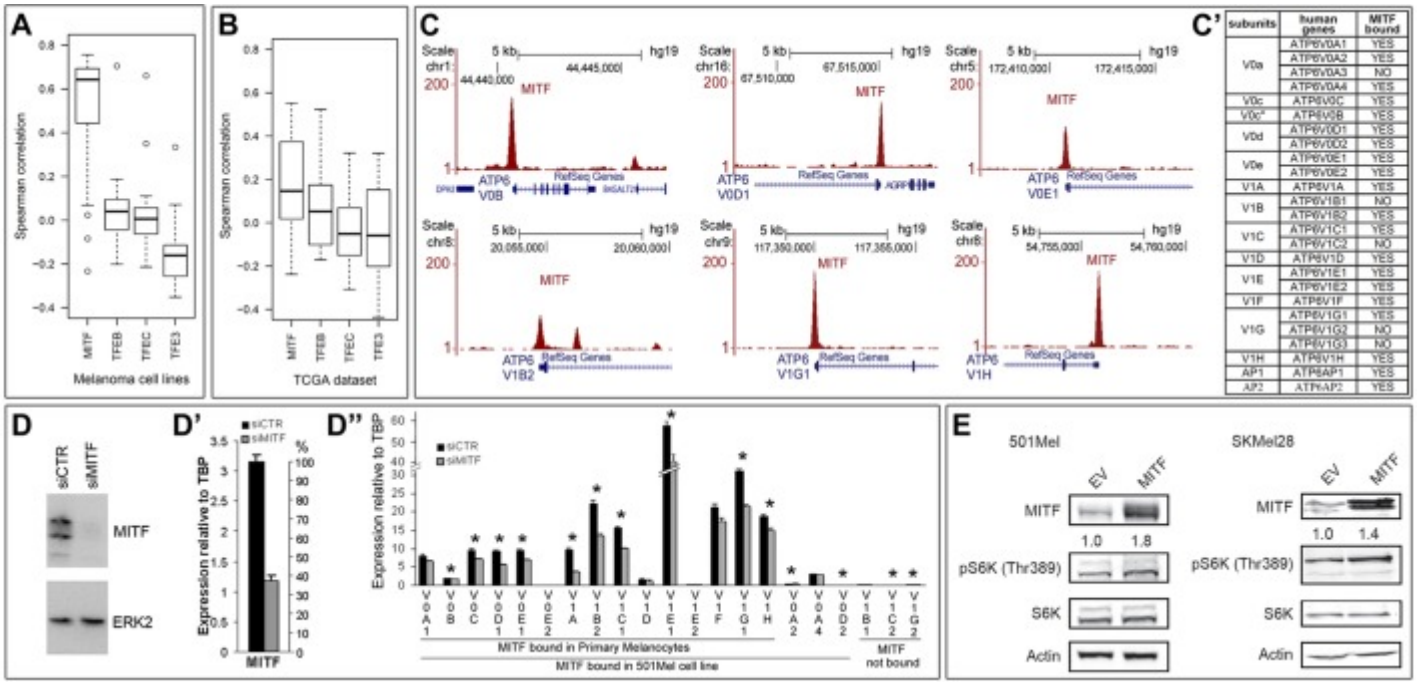

MITF controls v-ATPase subunit genes in human cells. (A,B) Boxplots of correlation (Kendall) coefficients between MiT genes (TFE3, TFEB, TFEC and MITF) and ATP6 genes in 24 melanoma cell lines (A) and 331 melanoma tumors (B). The box represents the 25–75th percentiles, and the median is indicated. The whiskers show the 10–90th percentiles. (C,C′) Direct binding of MITF to ATP6 genes in 501Mel cell line, including examples of MITF ChIP-Seq peaks at selected v-ATPase genes (C) and summary of results from ChIP-Seq analysis (C′); see supplementary material Table S6B for details. (D–D″) ATP6 gene regulation in response to downregulation of MITF by siRNA in 501Mel cells. (D) Cells were transfected with control siRNA (siCTR) or siRNA against MITF (siMITF) for 72 h before harvesting and analyzed by western blotting with the indicated antibody. (D′) Level of MITF mRNA (qPCR readings normalized to TBP) in siCTR or siMITF transfected 501Mel cells. Treatment with siMITF results in ∼60% decrease in MITF mRNA. (D″) Level of ATP6 mRNAs (qPCR readings normalized to TBP) in siMITF versus siCTR transfected 501Mel cells. Results are mean±s.e.m., *n*=3. (E) Upregulation of TORC1 activity by MITF in two MITF-inducible melanoma lines. Western blots show that the level of pS6K increases in response to MITF induction. Proteins detected by antibody are listed on the right. Numbers show relative band intensity compared to control set as 1. EV, empty

vector control. Actin protein was used for loading control.

Table 1.

Control of ATP6 genes in melanoma lines and melanocytes

Table 1. Control of ATP6 genes in melanoma lines and melanocytes

ATP6 Gene	MITF–ATP6 correlation in 24 melanoma lines	ChIP (in 501Mel cells)	Human primary melanocytes	siMITF effect (501Mel cells)	Expression (mammals)
ATP6AP2	Corr	Bound	Bound	ND	ND
ATP6V0A1	Corr	Bound	Bound	No effect	UBI
ATP6V0B	Corr	Bound	Bound	Down	UBI
ATP6V0C	Corr	Bound	Bound	Down	UBI
ATP6V0D1	Corr	Bound	Bound	Down	UBI
ATP6V0E1	Corr	Bound	Bound	Down	UBI
ATP6V0E2	Corr	Bound	Bound	No effect	R
ATP6V1A	Corr	Bound	Bound	Down	UBI
ATP6V1B2	Corr	Bound	Bound	Down	UBI
ATP6V1C1	Corr	Bound	Bound	Down	UBI
ATP6V1D	Corr	Bound	Bound	No effect	UBI
ATP6V1E1	Corr	Bound	Bound	Down	UBI
ATP6V1F	Corr	Bound	Bound	No effect	UBI
ATP6V1G1	Corr	Bound	Bound	Down	UBI
ATP6V1H	Corr	Bound	Bound	Down	UBI
ATP6V1E2	NC	Bound	Bound	No effect	R
ATP6V0A4	Corr	Bound	Not bound	No effect	R
ATP6V0A2	Corr	Bound	Not bound	Up	UBI
ATP6V0D2	Corr	Bound	Not bound	Up	R
ATP6AP1	Corr	Bound	Not bound	ND	ND
ATP6V1C2	Expression very low	Not bound	Not bound	Down	R
ATP6V1G3	Expression very low	Not bound	Not bound	ND	R
ATP6V1B1	NC	Not bound	Not bound	No effect	R
TCIRG1	NC	Not bound	Not bound	ND	R
ATP6V1G2	NegC	Not bound	Not bound	Down	R

Proposed targets of Mitf in melamoma cells and melanocytes are shown in bold. The expression in mammals is as described by Holliday, 2014, Lee, 2012 or Toei et al., 2010.
Corr, positive correlation; NC, no correlation; NegC, negative correlation; UBI, ubiquitous expression; R, restricted expression; ND, not determined.